7

Multilayer Film Applications

7.1 Multilayer Dielectric Structures at Oblique Incidence

Using the matching and propagation matrices for transverse fields that we discussed in Sec. 6.3, we derive here the layer recursions for multiple dielectric slabs at oblique incidence.

Fig. 7.1.1 shows such a multilayer structure. The layer recursions relate the various field quantities, such as the electric fields and the reflection responses, at the *left* of each interface.

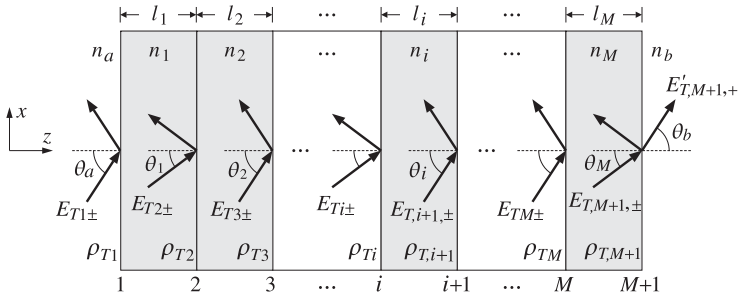

Fig. 7.1.1 Oblique incidence on multilayer dielectric structure.

We assume that there are no incident fields from the right side of the structure. The reflection/refraction angles in each medium are related to each other by Snell's law applied to each of the $M+1$ interfaces:

$$\boxed{n_a \sin\theta_a = n_i \sin\theta_i = n_b \sin\theta_b}, \quad i = 1, 2, \ldots, M \tag{7.1.1}$$

It is convenient also to define by Eq. (6.3.8) the propagation phases or *phase thicknesses* for each of the M layers, that is, the quantities $\delta_i = k_{zi} l_i$. Using $k_{zi} = k_0 n_i \cos\theta_i$, where k_0 is the free-space wavenumber, $k_0 = \omega/c_0 = 2\pi f/c_0 = 2\pi/\lambda$, we have for $i = 1, 2, \ldots, M$:

$$\boxed{\delta_i = \frac{\omega}{c_0} n_i l_i \cos\theta_i = \frac{2\pi}{\lambda} n_i l_i \cos\theta_i = \frac{2\pi}{\lambda} l_i n_i \sqrt{1 - \frac{n_a^2 \sin^2\theta_a}{n_i^2}}} \tag{7.1.2}$$

where we used Eq. (7.1.1) to write $\cos\theta_i = \sqrt{1-\sin^2\theta_i} = \sqrt{1 - n_a^2 \sin^2\theta_a / n_i^2}$. The transverse reflection coefficients at the $M+1$ interfaces are defined as in Eq. (5.1.1):

$$\rho_{Ti} = \frac{n_{T,i-1} - n_{Ti}}{n_{T,i-1} + n_{Ti}}, \quad i = 1, 2, \ldots, M+1 \tag{7.1.3}$$

where we set $n_{T0} = n_{Ta}$, as in Sec. 5.1. and $n_{T,M+1} = n_{Tb}$. The transverse refractive indices are defined in each medium by Eq. (6.2.13):

$$\boxed{n_{Ti} = \begin{cases} \dfrac{n_i}{\cos\theta_i}, & \text{TM polarization} \\ n_i \cos\theta_i, & \text{TE polarization} \end{cases}}, \qquad i = a, 1, 2, \ldots, M, b \tag{7.1.4}$$

To obtain the layer recursions for the electric fields, we apply the propagation matrix (6.3.5) to the fields at the left of interface $i+1$ and propagate them to the right of the interface i, and then, apply a matching matrix (6.3.11) to pass to the left of that interface:

$$\begin{bmatrix} E_{Ti+} \\ E_{Ti-} \end{bmatrix} = \frac{1}{\tau_{Ti}} \begin{bmatrix} 1 & \rho_{Ti} \\ \rho_{Ti} & 1 \end{bmatrix} \begin{bmatrix} e^{j\delta_i} & 0 \\ 0 & e^{-j\delta_i} \end{bmatrix} \begin{bmatrix} E_{T,i+1,+} \\ E_{T,i+1,-} \end{bmatrix}$$

Multiplying the matrix factors, we obtain:

$$\begin{bmatrix} E_{Ti+} \\ E_{Ti-} \end{bmatrix} = \frac{1}{\tau_{Ti}} \begin{bmatrix} e^{j\delta_i} & \rho_{Ti} e^{-j\delta_i} \\ \rho_{Ti} e^{j\delta_i} & e^{-j\delta_i} \end{bmatrix} \begin{bmatrix} E_{T,i+1,+} \\ E_{T,i+1,-} \end{bmatrix}, \quad i = M, M-1, \ldots, 1 \tag{7.1.5}$$

This is identical to Eqs. (5.1.2) with the substitutions $k_i l_i \to \delta_i$ and $\rho_i \to \rho_{Ti}$. The recursion is initialized at the left of the $(M+1)$st interface by performing an additional matching to pass to the right of that interface:

$$\begin{bmatrix} E_{T,M+1,+} \\ E_{T,M+1,-} \end{bmatrix} = \frac{1}{\tau_{T,M+1}} \begin{bmatrix} 1 & \rho_{T,M+1} \\ \rho_{T,M+1} & 1 \end{bmatrix} \begin{bmatrix} E'_{T,M+1,+} \\ 0 \end{bmatrix} \tag{7.1.6}$$

It follows now from Eq. (7.1.5) that the reflection responses, $\Gamma_{Ti} = E_{Ti-}/E_{Ti+}$, will satisfy the identical recursions as Eq. (5.1.5):

$$\boxed{\Gamma_{Ti} = \frac{\rho_{Ti} + \Gamma_{T,i+1} e^{-2j\delta_i}}{1 + \rho_{Ti} \Gamma_{T,i+1} e^{-2j\delta_i}}}, \quad i = M, M-1, \ldots, 1 \tag{7.1.7}$$

and initialized at $\Gamma_{T,M+1} = \rho_{T,M+1}$. Similarly, we obtain the following recursions for the total transverse electric and magnetic fields at each interface (they are continuous across each interface):

$$\begin{bmatrix} E_{Ti} \\ H_{Ti} \end{bmatrix} = \begin{bmatrix} \cos\delta_i & j\eta_{Ti} \sin\delta_i \\ j\eta_{Ti}^{-1} \sin\delta_i & \cos\delta_i \end{bmatrix} \begin{bmatrix} E_{T,i+1} \\ H_{T,i+1} \end{bmatrix}, \quad i = M, M-1, \ldots, 1 \tag{7.1.8}$$

where η_{Ti} are the transverse characteristic impedances defined by Eq. (6.2.12) and related to the refractive indices by $\eta_{Ti} = \eta_0/n_{Ti}$. The wave impedances, $Z_{Ti} = E_{Ti}/H_{Ti}$, satisfy the following recursions initialized by $Z_{T,M+1} = \eta_{Tb}$:

$$\boxed{Z_{Ti} = \eta_{Ti}\,\frac{Z_{T,i+1} + j\eta_{Ti}\tan\delta_i}{\eta_{Ti} + jZ_{T,i+1}\tan\delta_i}}, \quad i = M, M-1, \ldots, 1 \tag{7.1.9}$$

The MATLAB function `multidiel` that was introduced in Sec. 5.1 can also be used in the oblique case with two extra input arguments: the incidence angle from the left and the polarization type, TE or TM. Its full usage is as follows:

```
[Gamma1,Z1] = multidiel(n,L,lambda,theta,pol);      % multilayer dielectric structure
```

where `theta` is the angle $\theta = \theta_a$ and `pol` is one of the strings `'te'` or `'tm'`. If the angle and polarization arguments are omitted, the function defaults to normal incidence for which TE and TM are the same. The other parameters have the same meaning as in Sec. 5.1.

In using this function, it is convenient to normalize the wavelength λ and the optical lengths $n_i l_i$ of the layers to some reference wavelength λ_0. The frequency f will be normalized to the corresponding reference frequency $f_0 = c_0/\lambda_0$.

Defining the normalized thicknesses $L_i = n_i l_i/\lambda_0$, so that $n_i l_i = L_i \lambda_0$, and noting that $\lambda_0/\lambda = f/f_0$, we may write the phase thicknesses (7.1.2) in the normalized form:

$$\boxed{\delta_i = 2\pi\,\frac{\lambda_0}{\lambda}\,L_i\cos\theta_i = 2\pi\,\frac{f}{f_0}\,L_i\cos\theta_i}, \qquad i = 1, 2, \ldots, M \tag{7.1.10}$$

Typically, but not necessarily, the L_i are chosen to be quarter-wavelength long at λ_0, that is, $L_i = 1/4$. This way the same multilayer design can be applied equally well at microwave or at optical frequencies. Once the wavelength scale λ_0 is chosen, the physical lengths of the layers l_i can be obtained from $l_i = L_i\lambda_0/n_i$.

7.2 Lossy Multilayer Structures

The `multidiel` function can be revised to handle lossy media. The reflection response of the multilayer structure is still computed from Eq. (7.1.7) but with some changes. In Sec. 6.7 we discussed the general case when either one or both of the incident and transmitted media are lossy.

In the notation of Fig. 7.1.1, we may assume that the incident medium n_a is lossless and all the other ones, n_i, $i = 1, 2, \ldots, M, b$, are lossy (and nonmagnetic). To implement `multidiel`, one needs to know the real and imaginary parts of n_i as functions of frequency, that is, $n_i(\omega) = n_{Ri}(\omega) - jn_{Ii}(\omega)$, or equivalently, the complex dielectric constants of the lossy media:

$$\begin{aligned} \epsilon_i(\omega) &= \epsilon_{Ri}(\omega) - j\epsilon_{Ii}(\omega)\,, \quad i = 1, 2, \ldots, M, b \\ n_i(\omega) &= \sqrt{\frac{\epsilon_i(\omega)}{\epsilon_0}} = \sqrt{\frac{\epsilon_{Ri}(\omega) - j\epsilon_{Ii}(\omega)}{\epsilon_0}} = n_{Ri}(\omega) - jn_{Ii}(\omega) \end{aligned} \tag{7.2.1}$$

Snell's law given in Eq. (7.1.1) remains valid, except now the angles θ_i and θ_b are complex valued because n_i, n_b are. One can still define the transverse refractive indices n_{Ti} through Eq. (7.1.4) using the complex-valued n_i, and $\cos\theta_i$ given by:

$$\cos\theta_i = \sqrt{1 - \sin^2\theta_i} = \sqrt{1 - \frac{n_a^2\sin^2\theta_a}{n_i^2}}, \quad i = a, 1, 2 \ldots, M, b \tag{7.2.2}$$

The reflection coefficients defined in Eq. (7.1.3) are equivalent to those given in Eq. (6.7.2) for the case of arbitrary incident and transmitted media.

The phase thicknesses δ_i now become complex-valued and are given by $\delta_i = k_{zi} l_i$, where k_{zi} is computed as follows. From Snell's law we have $k_{xi} = k_{xa} = \omega\sqrt{\mu_0\epsilon_0}\,n_a \sin\theta_a = k_0 n_a \sin\theta_a$, where $k_0 = \omega\sqrt{\mu_0\epsilon_0} = \omega/c_0$ is the free-space wave number. Then,

$$k_{zi} = \sqrt{\omega^2\mu_0\epsilon_i - k_{xi}^2} = \frac{\omega}{c_0}\sqrt{n_i^2 - n_a^2\sin^2\theta_a}\,, \quad i = a, 1, \ldots, M, b \tag{7.2.3}$$

Thus, the complex phase thicknesses are given by:

$$\delta_i = k_{zi} l_i = \frac{\omega l_i}{c_0}\sqrt{n_i^2 - n_a^2\sin^2\theta_a}\,, \quad i = 1, 2, \ldots, M \tag{7.2.4}$$

Writing $c_0 = f_0\lambda_0$ for some reference frequency and wavelength, we may re-express (7.2.4) in terms of the normalized frequency and normalized physical lengths:

$$\delta_i = k_{zi} l_i = 2\pi\,\frac{f}{f_0}\,\frac{l_i}{\lambda_0}\sqrt{n_i^2 - n_a^2\sin^2\theta_a}\,, \quad i = 1, 2, \ldots, M \tag{7.2.5}$$

To summarize, given the complex $n_i(\omega)$ as in Eq. (7.2.1) at each desired value of ω, we calculate $\cos\theta_i$ from Eq. (7.2.2), n_{Ti} and ρ_{Ti} from Eqs. (7.1.4) and (7.1.3), and thicknesses δ_i from Eq. (7.2.5). Then, we use (7.1.7) to calculate the reflection response. The MATLAB function `multidiel2` implements these steps, with usage:

```
[Gamma1,Z1] = multidiel2(n,l,f,theta,pol);      % lossy multilayer structure
```

Once Γ_1 is determined, one may calculate the power entering each layer as well as the power lost within each layer. The time-averaged power per unit area entering the ith layer is the z-component of the Poynting vector, which is given in terms of the transverse E, H fields as follows:

$$\mathcal{P}_i = \frac{1}{2}\,\mathrm{Re}\left(E_{Ti}H_{Ti}^*\right), \quad i = 1, 2, \ldots, M \tag{7.2.6}$$

The power absorbed within the ith layer is equal to the difference of the power entering the layer and the power leaving it:

$$\mathcal{P}_i^{\text{loss}} = \mathcal{P}_i - \mathcal{P}_{i+1}\,, \quad i = 1, 2, \ldots, M \tag{7.2.7}$$

The transverse fields can be calculated by inverting the recursion (7.1.8), that is,

$$\begin{bmatrix} E_{T,i+1} \\ H_{T,i+1} \end{bmatrix} = \begin{bmatrix} \cos\delta_i & -j\eta_{Ti}\sin\delta_i \\ -j\eta_{Ti}^{-1}\sin\delta_i & \cos\delta_i \end{bmatrix} \begin{bmatrix} E_{Ti} \\ H_{Ti} \end{bmatrix}, \quad i = 1, 2, \ldots, M \tag{7.2.8}$$

The recursion is initialized with the fields E_{T1}, H_{T1} at the first interface. These can be calculated with the help of Γ_1:

$$\begin{aligned} E_{T1} &= E_{T1+} + E_{T1-} = E_{T1+}(1+\Gamma_1) \\ H_{T1} &= \frac{1}{\eta_{Ta}}(E_{T1+} - E_{T1-}) = \frac{1}{\eta_{Ta}} E_{T1+}(1-\Gamma_1) \end{aligned} \tag{7.2.9}$$

where $\eta_{Ta} = \eta_0/n_{Ta}$. The field E_{T1+} is the transverse component of the incident field. If we denote the total incident field by $E_{\rm in}$, then E_{T1+} will be given by:

$$E_{T1+} = \begin{cases} E_{\rm in}\,, & \text{TE case} \\ E_{\rm in}\cos\theta_a\,, & \text{TM case} \end{cases} \tag{7.2.10}$$

The total incident power (along the direction of the incident wave vector), its z-component, and the power entering the first layer will be given as follows (in both the TE and TM cases):

$$\mathcal{P}_{\rm in} = \frac{1}{2\eta_a}|E_{\rm in}|^2\,, \quad \mathcal{P}_{{\rm in},z} = \mathcal{P}_{\rm in}\cos\theta_a\,, \quad \mathcal{P}_1 = \mathcal{P}_{{\rm in},z}\left(1-|\Gamma_1|^2\right) \tag{7.2.11}$$

where $\eta_a = \eta_0/n_a$. Thus, one can start with $E_{\rm in} = \sqrt{2\eta_a \mathcal{P}_{\rm in}}$, if the incident power is known.

7.3 Single Dielectric Slab

Many features of oblique incidence on multilayer slabs can be clarified by studying the single-slab case, shown in Fig. 7.3.1. Assuming that the media to the left and right are the same, $n_a = n_b$, it follows that $\theta_b = \theta_a$ and also that $\rho_{T1} = -\rho_{T2}$. Moreover, Snell's law implies $n_a \sin\theta_a = n_1 \sin\theta_1$.

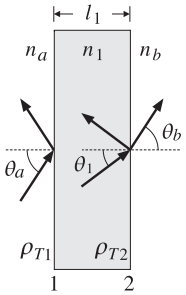

Fig. 7.3.1 Oblique incidence on single dielectric slab.

Because there are no incident fields from the right, the reflection response at the left of interface-2 is: $\Gamma_{T2} = \rho_{T2} = -\rho_{T1}$. It follows from Eq. (7.1.7) that the reflection response at the left of interface-1 will be:

$$\Gamma_{T1} = \frac{\rho_{T1} + \rho_{T2}e^{-2j\delta_1}}{1 + \rho_{T1}\rho_{T2}e^{-2j\delta_1}} = \frac{\rho_{T1}(1-e^{-2j\delta_1})}{1-\rho_{T1}^2 e^{-2j\delta_1}} \tag{7.3.1}$$

This is analogous to Eq. (4.5.4). According to Eq. (7.1.10), the phase thickness can be written in the following normalized form, where $L_1 = n_1 l_1/\lambda_0$:

$$\boxed{\delta_1 = 2\pi\frac{\lambda_0}{\lambda}L_1\cos\theta_1 = 2\pi\frac{f}{f_0}L_1\cos\theta_1 = \pi\frac{f}{f_1}} \tag{7.3.2}$$

$$\boxed{f_1 = \frac{f_0}{2L_1\cos\theta_1}} \tag{7.3.3}$$

At frequencies that are integral multiples of f_1, $f = mf_1$, the reflection response vanishes because $2\delta_1 = 2\pi(mf_1)/f_1 = 2\pi m$ and $e^{-2j\delta_1} = 1$. Similarly, at the half-integral multiples, $f = (m+0.5)f_1$, the response is maximum because $e^{-2j\delta_1} = -1$.

Because f_1 depends inversely on $\cos\theta_1$, then as the angle of incidence θ_a increases, $\cos\theta_1$ will decrease and f_1 will shift towards higher frequencies. The maximum shift will occur when θ_1 reaches its maximum refraction value $\theta_{1c} = \text{asin}(n_a/n_1)$ (assuming $n_a < n_1$.)

Similar shifts occur for the 3-dB width of the reflection response notches. By the same calculation that led to Eq. (4.5.9), we find for the 3-dB width with respect to the variable δ_1:

$$\tan\left(\frac{\Delta\delta_1}{2}\right) = \frac{1-\rho_{T1}^2}{1+\rho_{T1}^2}$$

Setting $\Delta\delta_1 = \pi\Delta f/f_1$, we solve for the 3-dB width in frequency:

$$\Delta f = \frac{2f_1}{\pi}\,\text{atan}\left(\frac{1-\rho_{T1}^2}{1+\rho_{T1}^2}\right) \tag{7.3.4}$$

The left/right bandedge frequencies are $f_1 \pm \Delta f/2$. The dependence of Δf on the incidence angle θ_a is more complicated here because ρ_{T1} also depends on it.

In fact, as θ_a tends to its grazing value $\theta_a \to 90^\circ$, the reflection coefficients for either polarization have the limit $|\rho_{T1}| \to 1$, resulting in zero bandwidth Δf. On the other hand, at the Brewster angle, $\theta_{aB} = \text{atan}(n_1/n_a)$, the TM reflection coefficient vanishes, resulting in maximum bandwidth. Indeed, because $\text{atan}(1) = \pi/4$, we have $\Delta f_{\max} = 2f_1\,\text{atan}(1)/\pi = f_1/2$.

Fig. 7.3.2 illustrates some of these properties. The refractive indices were $n_a = n_b = 1$ and $n_1 = 1.5$. The optical length of the slab was taken to be half-wavelength at the reference wavelength λ_0, so that $n_1 l_1 = 0.5\lambda_0$, or, $L_1 = 0.5$.

The graphs show the TE and TM reflectances $|\Gamma_{T1}(f)|^2$ as functions of frequency for the angles of incidence $\theta_1 = 75^\circ$ and $\theta_a = 85^\circ$. The normal incidence case is also included for comparison.

The corresponding refracted angles were $\theta_1 = \text{asin}\big(n_a \sin(\theta_a)/n_1\big) = 40.09^\circ$ and $\theta_1 = 41.62^\circ$. Note that the maximum refracted angle is $\theta_{1c} = 41.81^\circ$, and the Brewster angle, $\theta_{aB} = 56.31^\circ$.

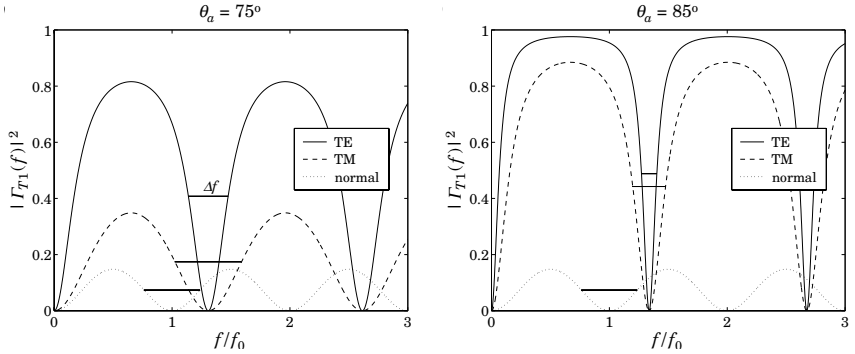

Fig. 7.3.2 TE and TM reflectances of half-wavelength slab.

The notch frequencies were $f_1 = f_0/(2L_1\cos\theta_1) = 1.31f_0$ and $f_1 = 1.34f_0$ for the angles $\theta_a = 75^o$ and 85^o. At normal incidence we have $f_1 = f_0/(2L_1) = f_0$, because $L_1 = 0.5$.

The graphs also show the 3-dB widths of the notches, calculated from Eq. (7.3.4). The reflection responses were computed with the help of the function `multidiel` with the typical MATLAB code:

```
na = 1; nb = 1;
n1 = 1.5; L1 = 0.5;

f = linspace(0,3,401);
theta = 75;

G0 = abs(multidiel([na,n1,nb], L1, 1./f)).^2;
Ge = abs(multidiel([na,n1,nb], L1, 1./f, theta, 'te')).^2;
Gm = abs(multidiel([na,n1,nb], L1, 1./f, theta, 'tm')).^2;
```

The shifting of the notch frequencies and the narrowing of the notch widths is evident from the graphs. Had we chosen $\theta_a = \theta_{aB} = 56.31^o$, the TM response would have been identically zero because of the factor ρ_{T1} in Eq. (7.3.1).

The single-slab case is essentially a simplified version of a Fabry-Perot interferometer [205], used as a spectrum analyzer. At multiples of f_1, there are narrow transmittance bands. Because f_1 depends on $f_0/\cos\theta_1$, the interferometer serves to separate different frequencies f_0 in the input by mapping them onto different angles θ_1.

7.4 Antireflection Coatings at Oblique Incidence

Antireflection coatings are typically designed for normal incidence and then used over a limited range of oblique incidence, such as up to about 30^o. As the angle of incidence increases, the antireflection band shifts towards lower wavelengths or higher frequencies. Any designed reflection zeros at normal incidence are no longer zeros at oblique incidence.

If a particular angle of incidence is preferred, it is possible to design the antireflection coating to match that angle. However, like the case of normal design, the effectiveness of this method will be over an angular width of approximately 30^o about the preferred angle.

To appreciate the effects of oblique incidence, we look at the angular behavior of our normal-incidence designs presented in Figs. 5.2.1 and 5.2.3.

The first example was a two-layer design with refractive indices $n_a = 1$ (air), $n_1 = 1.38$ (magnesium fluoride), $n_2 = 2.45$ (bismuth oxide), and $n_b = 1.5$ (glass). The designed normalized optical lengths of the layers were $L_1 = 0.3294$ and $L_2 = 0.0453$ at $\lambda_0 = 550$ nm.

Fig. 7.4.1 shows the TE and TM reflectances $|\Gamma_{T1}(\lambda)|^2$ as functions of λ, for the incidence angles $\theta = 0^o, 20^o, 30^o, 40^o$.

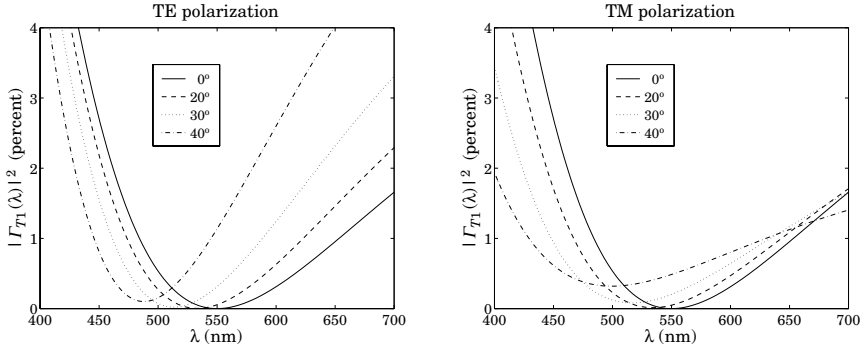

Fig. 7.4.1 Two-layer antireflection coating at oblique incidence.

We note the shifting of the responses towards lower wavelengths. The responses are fairly acceptable up to about 20^o–30^o. The typical MATLAB code used to generate these graphs was:

```
n = [1, 1.38, 2.45, 1.5]; L = [0.3294, 0.0453];
la0 = 550; la = linspace(400,700,101); pol='te';

G0  = abs(multidiel(n, L, la/la0)).^2 * 100;
G20 = abs(multidiel(n, L, la/la0, 20, pol)).^2 * 100;
G30 = abs(multidiel(n, L, la/la0, 30, pol)).^2 * 100;
G40 = abs(multidiel(n, L, la/la0, 40, pol)).^2 * 100;

plot(la, [G0; G20; G30; G40]);
```

As we mentioned above, the design can be matched at a particular angle of incidence. As an example, we choose $\theta_a = 30^o$ and redesign the two-layer structure.

The design equations are still (5.2.2) and (5.2.1), but with the replacement of n_i, ρ_i by their transverse values n_{Ti}, ρ_{Ti}, and the replacement of k_1l_1, k_2l_2 by the phase thicknesses at $\lambda = \lambda_0$, that is, $\delta_1 = 2\pi L_1\cos\theta_1$ and $\delta_2 = 2\pi L_2\cos\theta_2$. Moreover, we must choose to match the design either for TE or TM polarization.

Fig. 7.4.2 illustrates such a design. The upper left graph shows the TE reflectance matched at 30°. The designed optical thicknesses are in this case, $L_1 = 0.3509$ and $L_2 = 0.0528$. The upper right graph shows the corresponding TM reflectance, which cannot be matched simultaneously with the TE case.

The lower graphs show the same design, but now the TM reflectance is matched at 30°. The designed lengths were $L_1 = 0.3554$ and $L_2 = 0.0386$.

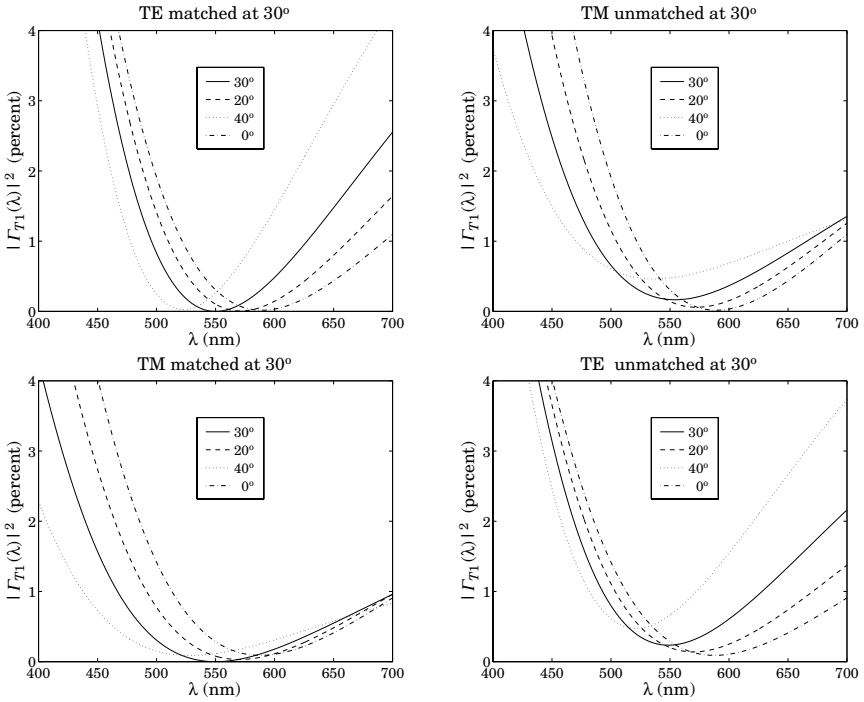

Fig. 7.4.2 Two-layer antireflection coating matched at 30 degrees.

The design steps are as follows. First, we calculate the refraction angles in all media from Eq. (7.1.1), $\theta_i = \text{asin}(n_a \sin\theta_a / n_i)$, for $i = a, 1, 2, b$. Then, assuming TE polarization, we calculate the TE refractive indices for all media $n_{Ti} = n_i \cos\theta_i$, $i = a, 1, 2, b$.

Then, we calculate the transverse reflection coefficients ρ_{Ti} from Eq. (7.1.3) and use them to solve Eq. (5.2.2) and (5.2.1) for the phase thicknesses δ_1, δ_2. Finally, we calculate the normalized optical lengths from $L_i = \delta_i / (2\pi \cos\theta_i)$, $i = 1, 2$. The following MATLAB code illustrates these steps:

```
n = [1, 1.38, 2.45, 1.5];
tha = 30;  thi = asin(na*sin(pi*tha/180)./n);

nt = n.*cos(thi);                    % for TM use nt = n./cos(thi)
r = n2r(nt);
```



```
c = sqrt((r(1)^2*(1-r(2)*r(3))^2 - (r(2)-r(3))^2)/(4*r(2)*r(3)*(1-r(1)^2)));
de2 = acos(c);
G2 = (r(2)+r(3)*exp(-2*j*de2))/(1 + r(2)*r(3)*exp(-2*j*de2));
de1 = (angle(G2) - pi - angle(r(1)))/2;
if de1 <0, de1 = de1 + 2*pi; end

L = [de1,de2]/2/pi;
L = L./cos(thi(2:3));

la0 = 550; la = linspace(400,700,401);

G30 = abs(multidiel(n, L, la/la0, 30, 'te')).^2 * 100;
G20 = abs(multidiel(n, L, la/la0, 20, 'te')).^2 * 100;
G40 = abs(multidiel(n, L, la/la0, 40, 'te')).^2 * 100;
G0  = abs(multidiel(n, L, la/la0)).^2 * 100;

plot(la, [G30; G20; G40; G0]);
```

Our second example in Fig. 5.2.3 was a quarter-half-quarter 3-layer design with refractive indices $n_1 = 1$ (air), $n_1 = 1.38$ (magnesium fluoride), $n_2 = 2.2$ (zirconium oxide), $n_3 = 1.63$ (cerium fluoride), and $n_b = 1.5$ (glass). The optical lengths of the layers were $L_1 = L_3 = 0.25$ and $L_2 = 0.5$.

Fig. 7.4.3 shows the TE and TM reflectances $|\Gamma_{T1}(\lambda)|^2$ as functions of λ, for the incidence angles $\theta = 0°, 20°, 30°, 40°$.

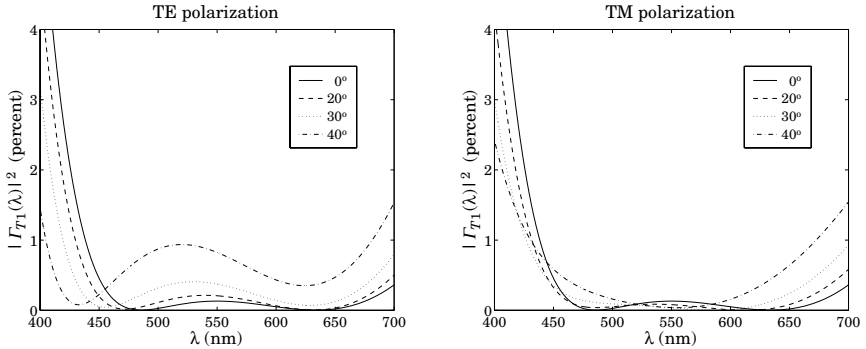

Fig. 7.4.3 Three-layer antireflection coating at oblique incidence.

The responses are fairly acceptable up to about 20°–30°, but are shifted towards lower wavelengths. The typical MATLAB code used to generate these graphs was:

```
n = [1, 1.38, 2.2, 1.63, 1.5]; L = [0.25, 0.50, 0.25];

la0 = 550; la = linspace(400,700,401);

G0  = abs(multidiel(n, L, la/la0)).^2 * 100;
G20 = abs(multidiel(n, L, la/la0, 20, 'te')).^2 * 100;
G30 = abs(multidiel(n, L, la/la0, 30, 'te')).^2 * 100;
G40 = abs(multidiel(n, L, la/la0, 40, 'te')).^2 * 100;

plot(la, [G0; G20; G30; G40]);
```

7.5 Omnidirectional Dielectric Mirrors

Until recently, it was generally thought that it was impossible to have an omnidirectional dielectric mirror, that is, a mirror that is perfectly reflecting at all angles of incidence and for both TE and TM polarizations. However, such mirrors are possible and have recently been manufactured [342,343] and the conditions for their existence clarified [342–346].

We consider the same dielectric mirror structure of Sec. 5.3, consisting of alternating layers of high and low index. Fig. 7.5.1 shows such a structure under oblique incidence. There are N bilayers and a total of $M = 2N + 1$ single layers, starting and ending with a high-index layer.

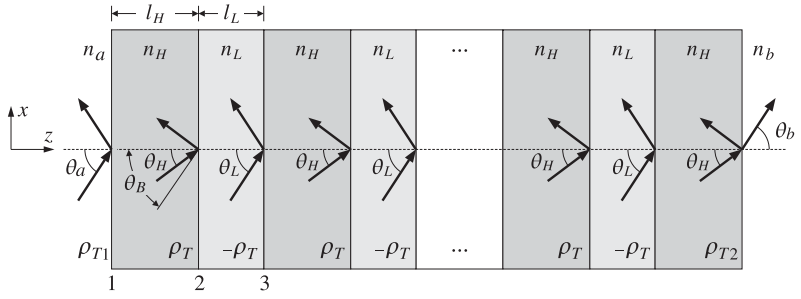

Fig. 7.5.1 Dielectric mirror at oblique incidence.

The incidence angles on each interface are related by Snell's law:

$$n_a \sin\theta_a = n_H \sin\theta_H = n_L \sin\theta_L = n_b \sin\theta_b \tag{7.5.1}$$

The phase thicknesses within the high- and low-index layers are in normalized form:

$$\boxed{\delta_H = 2\pi \frac{f}{f_0} L_H \cos\theta_H\,, \quad \delta_L = 2\pi \frac{f}{f_0} L_L \cos\theta_L} \tag{7.5.2}$$

where $L_H = n_H l_H/\lambda_0$, $L_L = n_L l_L/\lambda_0$ are the optical thicknesses normalized to some λ_0, and $f_0 = c_0/\lambda_0$. Note also, $\cos\theta_i = \sqrt{1 - n_a^2 \sin^2\theta_a / n_i^2}$, $i = H, L$.

A necessary (but not sufficient) condition for omnidirectional reflectivity for both polarizations is that the maximum angle of refraction $\theta_{H,\max}$ inside the first layer be less than the Brewster angle θ_B of the second interface, that is, the high-low interface, so that the Brewster angle can never be accessed by a wave incident on the first interface. If this condition is not satisfied, a TM wave would not be reflected at the second and all subsequent interfaces and will transmit through the structure.

Because $\sin\theta_{H,\max} = n_a/n_H$ and $\tan\theta_B = n_L/n_H$, or, $\sin\theta_B = n_L/\sqrt{n_H^2 + n_L^2}$, the condition $\theta_{H,\max} < \theta_B$, or the equivalent condition $\sin\theta_{H,\max} < \sin\theta_B$, can be written as $n_a/n_H < n_L/\sqrt{n_H^2 + n_L^2}$, or

$$\boxed{n_a < \frac{n_H n_L}{\sqrt{n_H^2 + n_L^2}}} \tag{7.5.3}$$

We note that the exact opposite of this condition is required in the design of multilayer Brewster polarizing beam splitters, discussed in the next section.

In addition to condition (7.5.3), in order to achieve omnidirectional reflectivity we must require that the high-reflectance bands have a *common* overlapping region for all incidence angles and for both polarizations.

To determine these bands, we note that the entire discussion of Sec. 5.3 carries through unchanged, provided we use the transverse reflection coefficients and transverse refractive indices. For example, the transverse version of the bilayer transition matrix of Eq. (5.3.5) will be:

$$F_T = \frac{1}{1-\rho_T^2} \begin{bmatrix} e^{j(\delta_H+\delta_L)} - \rho_T^2 e^{j(\delta_H-\delta_L)} & -2j\rho_T e^{-j\delta_H}\sin\delta_L \\ 2j\rho_T e^{j\delta_H}\sin\delta_L & e^{-j(\delta_H+\delta_L)} - \rho_T^2 e^{-j(\delta_H-\delta_L)} \end{bmatrix} \tag{7.5.4}$$

where $\rho_T = (n_{HT} - n_{LT})/(n_{HT} + n_{LT})$ and:

$$n_{HT} = \begin{cases} \dfrac{n_H}{\cos\theta_H} \\ n_H \cos\theta_H \end{cases} \qquad n_{LT} = \begin{cases} \dfrac{n_L}{\cos\theta_L} & \text{(TM polarization)} \\ n_L \cos\theta_L & \text{(TE polarization)} \end{cases} \tag{7.5.5}$$

Explicitly, we have for the two polarizations:

$$\rho_{TM} = \frac{n_H \cos\theta_L - n_L \cos\theta_H}{n_H \cos\theta_L + n_L \cos\theta_H}\,, \quad \rho_{TE} = \frac{n_H \cos\theta_H - n_L \cos\theta_L}{n_H \cos\theta_H + n_L \cos\theta_L} \tag{7.5.6}$$

The trace of F_T is as in Eq. (5.3.13):

$$\boxed{a = \frac{\cos(\delta_H + \delta_L) - \rho_T^2 \cos(\delta_H - \delta_L)}{1 - \rho_T^2}} \tag{7.5.7}$$

The eigenvalues of the matrix F_T are $\lambda_\pm = e^{\pm jKl}$, where $K = \text{acos}(a)/l$ and $l = l_H + l_L$. The condition $a = -1$ determines the bandedge frequencies of the high-reflectance bands. As in Eq. (5.3.16), this condition is equivalent to:

$$\boxed{\cos^2\left(\frac{\delta_H + \delta_L}{2}\right) = \rho_T^2 \cos^2\left(\frac{\delta_H - \delta_L}{2}\right)} \tag{7.5.8}$$

Defining the quantities $L_\pm = L_H \cos\theta_H \pm L_L \cos\theta_L$ and the normalized frequency $F = f/f_0$, we may write:

$$\frac{\delta_H \pm \delta_L}{2} = \pi \frac{f}{f_0}\,(L_H \cos\theta_H \pm L_L \cos\theta_L) = \pi F L_\pm \tag{7.5.9}$$

Then, taking square roots of Eq. (7.5.8), we have:

$$\cos(\pi F L_+) = \pm|\rho_T| \cos(\pi F L_-)$$

The plus sign gives the left bandedge, $F_1 = f_1/f_0$, and the minus sign, the right bandedge, $F_2 = f_2/f_0$. Thus, F_1, F_2 are the solutions of the equations:

$$\boxed{\begin{aligned}\cos(\pi F_1 L_+) &= |\rho_T|\cos(\pi F_1 L_-)\\ \cos(\pi F_2 L_+) &= -|\rho_T|\cos(\pi F_2 L_-)\end{aligned}} \tag{7.5.10}$$

The bandwidth and center frequency of the reflecting band are:

$$\boxed{\frac{\Delta f}{f_0} = \Delta F = F_2 - F_1\,, \qquad \frac{f_c}{f_0} = F_c = \frac{F_1+F_2}{2}} \tag{7.5.11}$$

The corresponding bandwidth in wavelengths is defined in terms of the left and right bandedge wavelengths:

$$\boxed{\lambda_1 = \frac{\lambda_0}{F_2} = \frac{c_0}{f_2}\,, \qquad \lambda_2 = \frac{\lambda_0}{F_1} = \frac{c_0}{f_1}\,, \qquad \Delta\lambda = \lambda_2 - \lambda_1} \tag{7.5.12}$$

An approximate solution of Eq. (7.5.10) can be obtained by setting $L_- = 0$ in the right-hand sides of Eq. (7.5.10):

$$\cos(\pi F_1 L_+) = |\rho_T|\,, \quad \cos(\pi F_2 L_+) = -|\rho_T| \tag{7.5.13}$$

with solutions:

$$F_1 = \frac{\operatorname{acos}(|\rho_T|)}{\pi L_+}\,, \quad F_2 = \frac{\operatorname{acos}(-|\rho_T|)}{\pi L_+} \tag{7.5.14}$$

Using the trigonometric identities $\operatorname{acos}(\pm|\rho_T|) = \pi/2 \mp \operatorname{asin}(|\rho_T|)$, we obtain the bandwidth and center frequency:

$$\boxed{\Delta f = f_2 - f_1 = \frac{2f_0 \operatorname{asin}(|\rho_T|)}{\pi L_+}\,, \qquad f_c = \frac{f_1+f_2}{2} = \frac{f_0}{2L_+}} \tag{7.5.15}$$

It follows that the center wavelength will be $\lambda_c = c_0/f_c = 2L_+\lambda_0$ or,

$$\boxed{\lambda_c = 2L_+\lambda_0 = 2(l_H n_H \cos\theta_H + l_L n_L \cos\theta_L)} \tag{7.5.16}$$

At normal incidence, we have $\lambda_c = 2(l_H n_H + l_L n_L)$. For quarter-wavelength designs at λ_0 at normal incidence, we have $L_+ = 1/4 + 1/4 = 1/2$, so that $\lambda_c = \lambda_0$.

The accuracy of the approximate solution (7.5.14) depends on the ratio $d = L_-/L_+$. Even if at normal incidence the layers were quarter-wavelength with $L_H = L_L = 0.25$, the equality of L_H and L_L will no longer be true at other angles of incidence. In fact, the quantity d is an increasing function of θ_a. For larger values of d, the exact solution of (7.5.10) can be obtained by the following iteration:

$$\boxed{\begin{aligned}&\text{initialize with } F_1 = F_2 = 0,\\ &\text{for } i = 0, 1, \ldots, N_{\text{iter}}, \text{ do:}\\ &\quad F_1 = \frac{1}{\pi L_+}\operatorname{acos}\big(|\rho_T|\cos(\pi F_1 L_-)\big)\\ &\quad F_2 = \frac{1}{\pi L_+}\operatorname{acos}\big(-|\rho_T|\cos(\pi F_2 L_-)\big)\end{aligned}} \tag{7.5.17}$$

Evidently, the $i = 0$ iteration gives the zeroth-order solution (7.5.14). The iteration converges extremely fast, requiring only 3–4 iterations N_{iter}. The MATLAB function `omniband` implements this algorithm. It has usage:

```
[F1,F2] = omniband(na,nH,nL,LH,LL,theta,pol,Niter)     % bandedge frequencies
[F1,F2] = omniband(na,nH,nL,LH,LL,theta,pol)           % equivalent to Nbiter = 0
```

where `theta` is the incidence angle in degrees, `pol` is one of the strings `'te'` or `'tm'` for TE or TM polarization, and `Niter` is the desired number of iterations. If this argument is omitted, only the $i = 0$ iteration is carried out.

It is straightforward but tedious to verify the following facts about the above solutions. First, f_1, f_2 are *increasing* functions of θ_a for both TE and TM polarizations. Thus, the center frequency of the band $f_c = (f_1+f_2)/2$ shifts towards higher frequencies with increasing angle θ_a. The corresponding wavelength intervals will shift towards lower wavelengths.

Second, the bandwidth $\Delta f = f_2 - f_1$ is an increasing function of θ_a for TE, and a decreasing one for TM polarization. Thus, as θ_a increases, the reflecting band for TE *expands* and that of TM *shrinks*, while their (slightly different) centers f_c shift upwards.

In order to achieve omnidirectional reflectivity, the TE and TM bands must have a common overlapping intersection for all angles of incidence. Because the TM band is always narrower than the TE band, it will determine the final common omnidirectional band.

The worst case of overlap is for the TM band at 90° angle of incidence, which must overlap with the TM/TE band at 0°. The left bandedge of this TM band, $f_{1,TM}(90^\circ)$, must be *less* than the right bandedge of the 0° band, $f_2(0^\circ)$. This is a sufficient condition for omnidirectional reflectivity.

Thus, the minimum band shared by all angles of incidence and both polarizations will be $[f_{1,TM}(90^\circ),\, f_2(0^\circ)]$, having width:

$$\boxed{\Delta f_{\min} = f_2(0^\circ) - f_{1,TM}(90^\circ)} \quad \text{(minimum omnidirectional bandwidth)} \tag{7.5.18}$$

In a more restricted sense, the common reflecting band for both polarizations and for angles up to a given θ_a will be $[f_{1,TM}(\theta_a),\, f_{2,TM}(0^\circ)]$ and the corresponding bandwidth:

$$\Delta f(\theta_a) = f_2(0^\circ) - f_{1,TM}(\theta_a) \tag{7.5.19}$$

In addition to computing the bandwidths of either the TM or the TE bands at any angle of incidence, the function `omniband` can also compute the above common bandwidths. If the parameter `pol` is equal to `'tem'`, then F_1, F_2 are those of Eqs. (7.5.18) and (7.5.19). Its extended usage is as follows:

```
[F1,F2] = omniband(na,nH,nL,LH,LL,theta,'tem')      % Eq. (7.5.19)
[F1,F2] = omniband(na,nH,nL,LH,LL,90,'tem')         % Eq. (7.5.18)
[F1,F2] = omniband(na,nH,nL,LH,LL)                  % Eq. (7.5.18)
```

Next, we discuss some simulation examples that will help clarify the above remarks.

Example 7.5.1: The first example is the angular dependence of Example 5.3.2. In order to flatten out and sharpen the edges of the reflecting bands, we use $N = 30$ bilayers. Fig. 7.5.2 shows the TE and TM reflectances $|\Gamma_{T1}(\lambda)|^2$ as functions of the free-space wavelength λ, for the two angles of incidence $\theta_a = 45^o$ and 80^o.

Fig. 7.5.3 depicts the reflectances as functions of frequency f. The refractive indices were $n_a = 1$, $n_H = 2.32$, $n_L = 1.38$, $n_b = 1.52$, and the bilayers were quarter-wavelength $L_H = L_L = 0.25$ at the normalization wavelength $\lambda_0 = 500$ nm.

The necessary condition (7.5.3) is satisfied and we find for the maximum angle of refraction and the Brewster angle: $\theta_{H,\max} = 25.53^o$ and $\theta_B = 30.75^o$ Thus, we have $\theta_{H,\max} < \theta_B$.

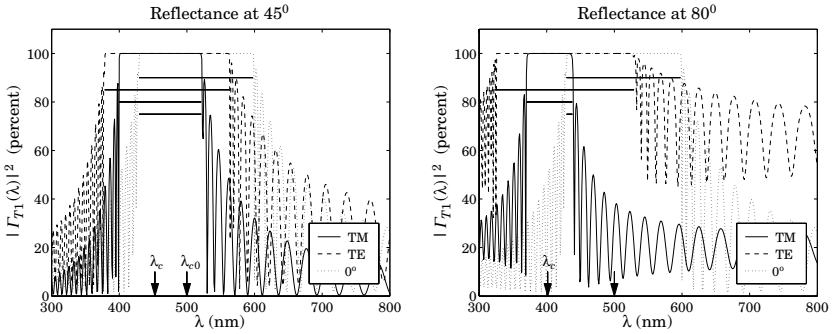

Fig. 7.5.2 TM and TE reflectances for $n_H = 2.32$, $n_L = 1.38$.

On each graph, we have indicated the corresponding bandwidth intervals calculated with `omniband`. The indicated intervals are for 0^o incidence, for TE and TM, and for the common band Eq. (7.5.19) at θ_a. We observe the shifting of the bands towards higher frequencies, or lower wavelengths, and the shrinking of the TM and expanding of the TE bands, and the shrinking of the common band.

At 45^o, there is still sufficient overlap, but at 80^o, the TM band has shifted almost to the end of the 0^o band, resulting in an extremely narrow common band.

The arrows labeled f_{c0} and f_c represent the (TM) band center frequencies at 0^o and 45^o or 80^o. The calculated bandedges corresponding to 90^o incidence were $\lambda_1 = \lambda_0/F_{2,TM}(0^o) = 429.73$ nm and $\lambda_2 = \lambda_0/F_{1,TM}(90^o) = 432.16$ nm, with bandwidth $\Delta\lambda = \lambda_2 - \lambda_1 = 2.43$ nm. Thus, this structure does exhibit omnidirectional reflectivity, albeit over a very narrow band. The MATLAB code used to generate these graphs was:

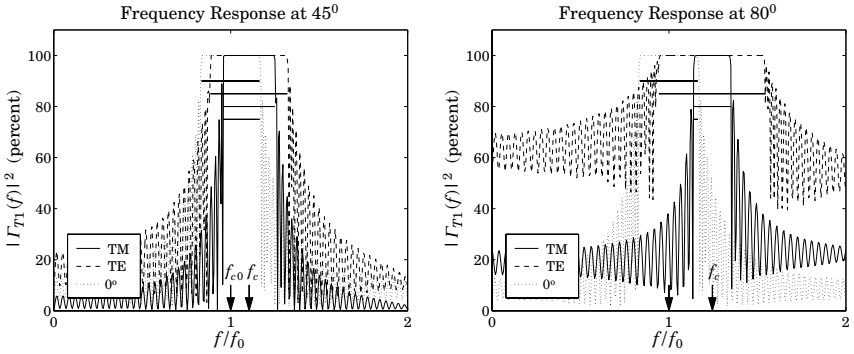

Fig. 7.5.3 TM and TE frequency responses for $n_H = 2.32$, $n_L = 1.38$.

```
na = 1; nb = 1.52; nH = 2.32; nL = 1.38;
LH = 0.25; LL = 0.25;

la0 = 500;
la = linspace(300,800,501);

th = 45; N = 30;
n = [na, nH, repmat([nL,nH], 1, N), nb];
L = [LH, repmat([LL,LH], 1, N)];
Ge = 100*abs(multidiel(n,L,la/la0, th, 'te')).^2;
Gm = 100*abs(multidiel(n,L,la/la0, th, 'tm')).^2;
G0 = 100*abs(multidiel(n,L,la/la0)).^2;

plot(la,Gm, la,Ge, la,G0);

[F10,F20] = omniband(na,nH,nL,LH,LL, 0, 'te');
[F1e,F2e] = omniband(na,nH,nL,LH,LL, th,'te');
[F1m,F2m] = omniband(na,nH,nL,LH,LL, th,'tm');
[F1,F2] =   omniband(na,nH,nL,LH,LL, th,'tem');
```

Because the reflectivity bands shrink with decreasing ratio n_H/n_L, if we were to slightly decrease n_H, then the TM band could be made to shift beyond the end of the 0^o band and there would be no common overlapping reflecting band for all angles. We can observe this behavior in Fig. 7.5.4, which has $n_H = 2$, with all the other parameters kept the same.

At 45^o there is a common overlap, but at 80^o, the TM band has already moved beyond the 0^o band, while the TE band still overlaps with the latter. This example has no omnidirectional reflectivity, although the necessary condition (7.5.3) is still satisfied with $\theta_{H,\max} = 30^o$ and $\theta_B = 34.61^o$.

On the other hand, if we were to increase n_H, all the bands will widen, and so will the final common band, resulting in an omnidirectional mirror of wider bandwidth. Fig. 7.5.5 shows the case of $n_H = 3$, exhibiting a substantial overlap and omnidirectional behavior.

The minimum band (7.5.18) was $[F_1, F_2] = [1.0465, 1.2412]$ corresponding to the wavelength bandedges $\lambda_1 = \lambda_0/F_2 = 402.84$ nm and $\lambda_2 = \lambda_0/F_1 = 477.79$ nm with a width of $\Delta\lambda = \lambda_2 - \lambda_1 = 74.95$ nm, a substantial difference from that of Fig. 7.5.2. The bandedges

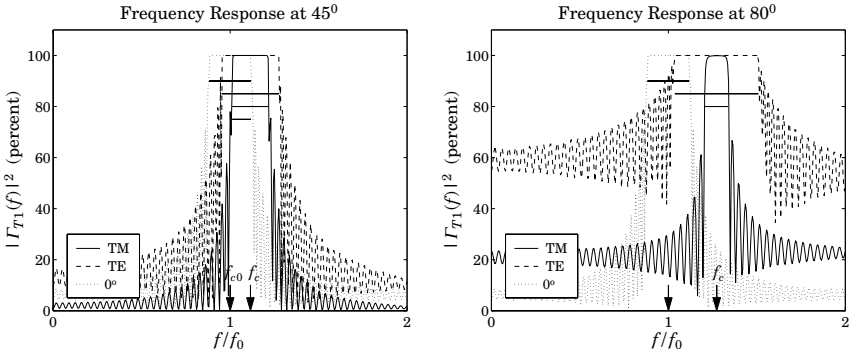

Fig. 7.5.4 TM and TE reflectances for $n_H = 2$, $n_L = 1.38$.

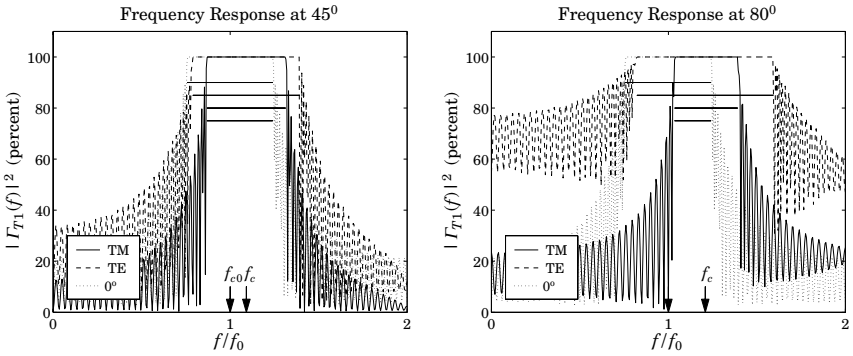

Fig. 7.5.5 TM and TE reflectances for $n_H = 3$, $n_L = 1.38$.

were computed with $N_{\text{it}} = 0$ in Eq. (7.5.17); with $N_{\text{it}} = 3$, we obtain the more accurate values: $[F_1, F_2] = [1.0505, 1.2412]$.

To illustrate the dependence of the TE and TM bandwidths on the incident angle θ_a, we have calculated and plotted the normalized bandedge frequencies $F_1(\theta_a)$, $F_2(\theta_a)$ for the range of angles $0 \le \theta_a \le 90^\circ$ for both polarizations. The left graph of Fig. 7.5.6 shows the case $n_H = 3$, $n_L = 1.38$, and the right graph, the case $n_H = 2$, $n_L = 1.38$.

We note that the TE band widens with increasing angle, whereas the TM band narrows. At the same time, the band centers move toward higher frequencies. In the left graph, there is a common band shared by both polarizations and all angles, that is, the band defined by $F_2(0^\circ)$, and $F_{1,\text{TM}}(90^\circ)$. For the right graph, the bandedge $F_{1,\text{TM}}(\theta_a)$ increases beyond $F_2(0^\circ)$ for angles θ_a greater than about 61.8°, and therefore, there is no omnidirectional band. The calculations of $F_1(\theta_a)$, $F_2(\theta_a)$ were done with `omniband` with $N_{\text{iter}} = 3$. □

Example 7.5.2: In Fig. 7.5.7, we study the effect of changing the optical lengths of the bilayers from quarter-wavelength to $L_H = 0.3$ and $L_L = 0.1$. The main result is to narrow the bands. This example, also illustrates the use of the iteration (7.5.17). The approximate

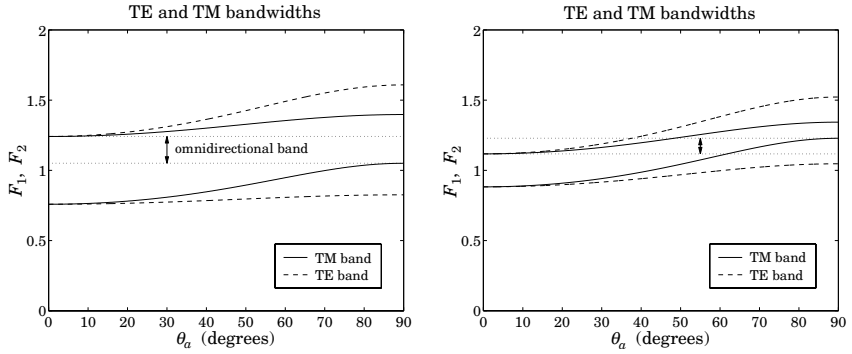

Fig. 7.5.6 TM/TE bandgaps versus angle for $n_H = 3$, $n_L = 1.38$ and $n_H = 2$, $n_L = 1.38$.

solution (7.5.15) and exact solutions for the 80° bandedge frequencies are obtained from the two MATLAB calls:

```
[F1,F2] = omniband(na,nH,nL,LH,LL,80,'tem',0);
[F1,F2] = omniband(na,nH,nL,LH,LL,80,'tem',3);
```

with results $[F_1, F_2] = [1.0933, 1.3891]$ and $[F_1, F_2] = [1.1315, 1.3266]$, respectively. Three iterations produce an excellent approximation to the exact solution. □

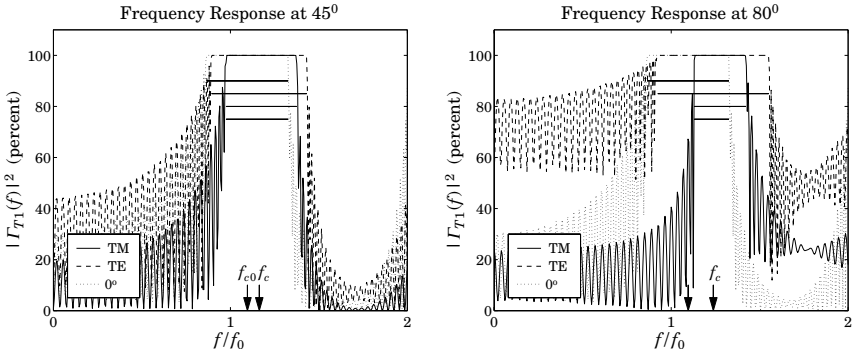

Fig. 7.5.7 Unequal length layers $L_H = 0.30$, $L_L = 0.15$.

Example 7.5.3: Here, we revisit Example 5.3.3, whose parameters correspond to the recently constructed omnidirectional infrared mirror [342]. Fig. 7.5.8 shows the reflectances as functions of wavelength and frequency at $\theta_a = 45^\circ$ and 80° for both TE and TM polarizations. At both angles of incidence there is a wide overlap, essentially over the desired 10–15 μm band.

The structure consisted of nine alternating layers of Tellurium ($n_H = 4.6$) and Polystyrene ($n_L = 1.6$) on a NaCl substrate ($n_b = 1.48$.) The physical lengths were $l_H = 0.8$ and $l_L = 1.6$ μm. The normalizing wavelength was $\lambda_0 = 12.5$ μm. The optical thicknesses in units of λ_0 were $L_H = 0.2944$ and $L_L = 0.2112$.

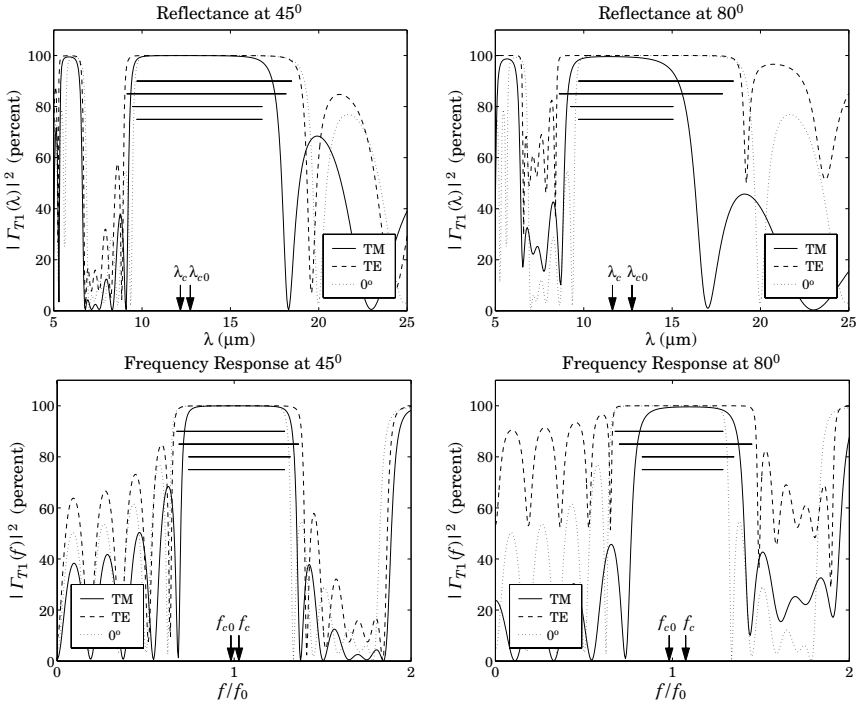

Fig. 7.5.8 Nine-layer Te/PS omnidirectional mirror over the infrared.

The bandedges at 0º were $[F_1, F_2] = [0.6764, 1.2875]$ with center frequency $F_{c0} = 0.9819$, corresponding to wavelength $\lambda_{c0} = \lambda_0/F_{c0} = 12.73$ μm. Similarly, at 45º, the band centers for TE and TM polarizations were $F_{c,TE} = 1.0272$ and $F_{c,TM} = 1.0313$, resulting in the wavelengths $\lambda_{c,TE} = 12.17$ and $\lambda_{c,TM} = 12.12$ μm (shown on the graphs are the TE centers only.)

The final bandedges of the common reflecting band computed from Eq. (7.5.18) were $[F_1, F_2] = [0.8207, 1.2875]$, resulting in the wavelength bandedges $\lambda_1 = \lambda_0/F_2 = 9.71$ and $\lambda_2 = \lambda_0/F_1 = 14.95$ μm, with a width of $\Delta\lambda = \lambda_2 - \lambda_1 = 5.24$ μm and band center $(\lambda_1 + \lambda_2)/2 = 12.33$ μm (the approximation (7.5.15) gives 5.67 and 12.4 μm.) The graphs were generated by the following MATLAB code:

```
la0 = 12.5; la = linspace(5,25,401);
na = 1; nb = 1.48; nH = 4.6; nL = 1.6;
lH = 0.8; lL = 1.65;  LH = nH*lH/la0; LL = nL*lL/la0;

th = 45;
```



```
N = 4;
n = [na, nH, repmat([nL,nH], 1, N), nb];
L = [LH, repmat([LL,LH], 1, N)];
Ge = 100*abs(multidiel(n,L,la/la0, th, 'te')).^2;
Gm = 100*abs(multidiel(n,L,la/la0, th, 'tm')).^2;
G0 = 100*abs(multidiel(n,L,la/la0)).^2;

plot(la,Gm, la,Ge, la,G0);

Ni = 5;
[F10,F20] = omniband(na,nH,nL,LH,LL, 0, 'te', Ni);      band at 0º
[F1e,F2e] = omniband(na,nH,nL,LH,LL, th,'te', Ni);      TE band
[F1m,F2m] = omniband(na,nH,nL,LH,LL, th,'tm', Ni);      TM band
[F1,F2]   = omniband(na,nH,nL,LH,LL, th,'tem',Ni);      Eq. (7.5.19)
[F1,F2]   = omniband(na,nH,nL,LH,LL, 90,'tem',Ni);      Eq. (7.5.18)
```

Finally, Fig. 7.5.9 shows the same example with the number of bilayers doubled to $N = 8$. The mirror bands are flatter and sharper, but the widths are the same. □

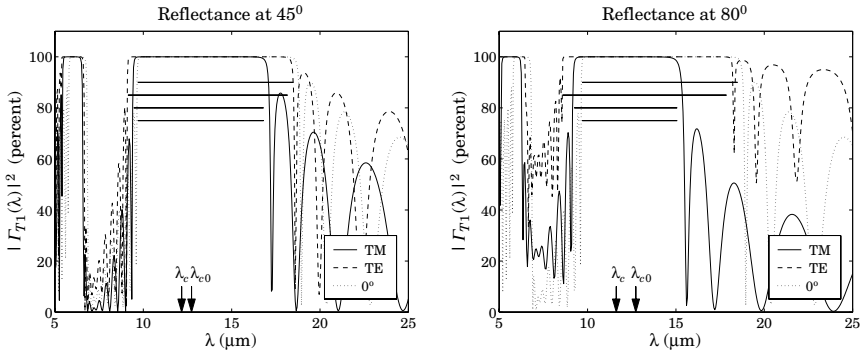

Fig. 7.5.9 Omnidirectional mirror with $N = 8$.

Example 7.5.4: The last example has parameters corresponding to the recently constructed omnidirectional reflector over the visible range [343]. The refractive indices were $n_a = 1$, $n_H = 2.6$ (ZnSe), $n_L = 1.34$ (Na_3AlF_6 cryolite), and $n_b = 1.5$ (glass substrate.) The layer lengths were $l_H = l_L = 90$ nm. There were $N = 9$ bilayers or $2N + 1 = 19$ layers, starting and ending with n_H.

With these values, the maximum angle of refraction is $\theta_{H,\max} = 22.27^o$ and is less than the Brewster angle $\theta_B = 27.27^o$.

The normalizing wavelength was taken to be $\lambda_0 = 620$ nm. Then, the corresponding optical lengths were $L_L = n_L l_L/\lambda_0 = 0.1945$ and $L_H = n_H l_H/\lambda_0 = 0.3774$. The overall minimum omnidirectional band is $[\lambda_1, \lambda_2] = [605.42, 646.88]$ nm. It was computed by the MATLAB call to `omniband` with $N_i = 5$ iterations:

```
[F1,F2] = omniband(na,nH,nL,LH,LL,90,'tem',Ni);
la1 = la0/F2; la2 = la0/F1;
```

(The values of λ_1, λ_2 do not depend on the choice of λ_0.) Fig. 7.5.10 shows the reflectance at 45° and 80°. The upper panel of graphs has $N = 9$ bilayers as in [343]. The lower panel has $N = 18$ bilayers or 38 layers, and has more well-defined band gaps. The two arrows in the figures correspond to the values of λ_1, λ_2 of the minimum omnidirectional band. □

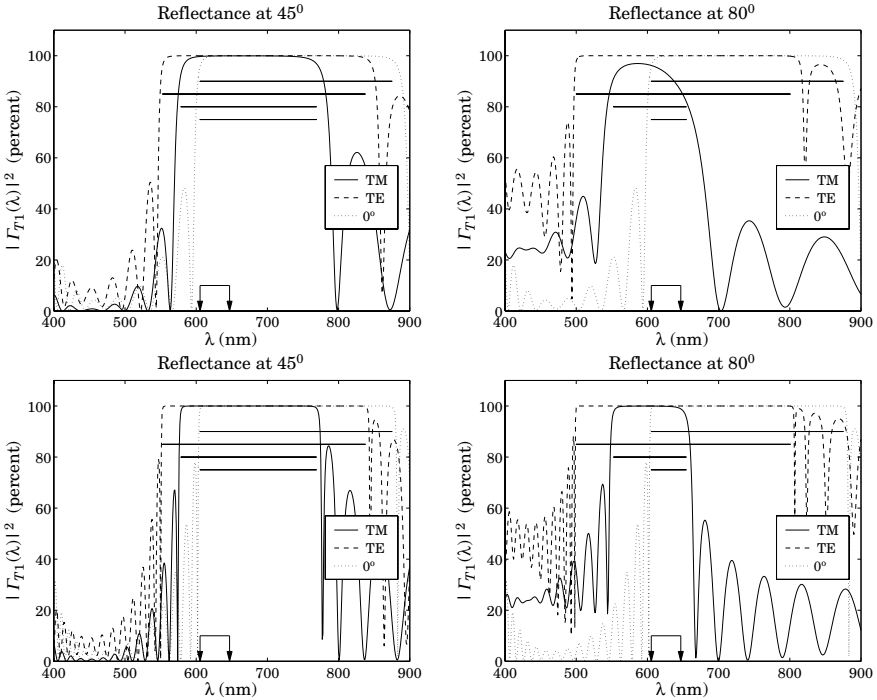

Fig. 7.5.10 Omnidirectional mirror over visible band.

7.6 Polarizing Beam Splitters

The objective of an omnidirectional mirror is to achieve high reflectivity for both polarizations. However, in polarizers, we are interested in separating the TE and TM polarizations. This can be accomplished with a periodic bilayer structure of the type shown in Fig. 7.5.1, which is highly reflecting only for TE and highly transmitting for TM polarizations. This is the principle of the so-called MacNeille polarizers [207,211,214,233,236,251–257].

If the angle of incidence θ_a is chosen such that the angle of refraction in the first high-index layer is equal to the Brewster angle of the high-low interface, then the TM component will not be reflected at the bilayer interfaces and will transmit through. The design condition is $\theta_H = \theta_B$, or $\sin\theta_H = \sin\theta_B$, which gives:

$$n_a \sin\theta_a = n_H \sin\theta_H = n_H \sin\theta_B = \frac{n_H n_L}{\sqrt{n_H^2 + n_L^2}} \tag{7.6.1}$$

This condition can be solved either for the angle θ_a or for the index n_a of the incident medium:

$$\sin\theta_a = \frac{n_H n_L}{n_a \sqrt{n_H^2 + n_L^2}} \quad \text{or,} \quad n_a = \frac{n_H n_L}{\sin\theta_a \sqrt{n_H^2 + n_L^2}} \tag{7.6.2}$$

In either case, the feasibility of this approach requires the opposite of the condition (7.5.3), that is,

$$n_a > \frac{n_H n_L}{\sqrt{n_H^2 + n_L^2}} \tag{7.6.3}$$

If the angle θ_a is set equal to the convenient value of 45°, then, condition Eq. (7.6.2) fixes the value of the refractive index n_a to be given by:

$$n_a = \frac{\sqrt{2}\, n_H n_L}{\sqrt{n_H^2 + n_L^2}} \tag{7.6.4}$$

Fig. 7.6.1 depicts such a multilayer structure sandwiched between two glass prisms with 45° angles. The thin films are deposited along the hypotenuse of each prism and the prisms are then cemented together. The incident, reflected, and transmitted beams are perpendicular to the prism sides.

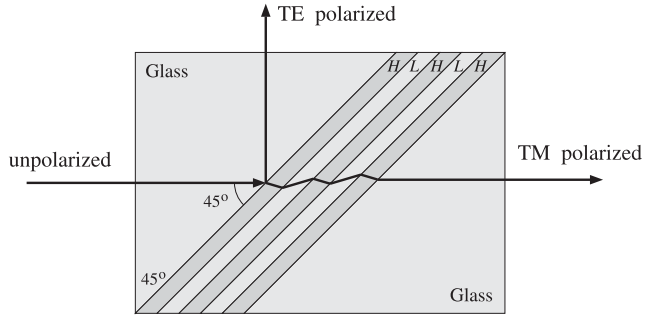

Fig. 7.6.1 Polarizing beam splitter.

Not many combinations of available materials satisfy condition (7.6.4). One possible solution is Banning's [214] with $n_H = 2.3$ (zinc sulfide), $n_L = 1.25$ (cryolite), and $n_a = 1.5532$. Another solution is given in Clapham, et al, [236], with $n_H = 2.04$ (zirconium oxide), $n_L = 1.385$ (magnesium fluoride), and $n_a = 1.6205$ (a form of dense flint glass.)

Fig. 7.6.2 shows the TE and TM reflectances of the case $n_H = 2.3$ and $n_L = 1.25$. The incident and output media had $n_a = n_b = 1.5532$. The maximum reflectivity for the TE

component is 99.99%, while that of the TM component is 3% (note the different vertical scales in the two graphs.)

The number of bilayers was $N = 5$ and the center frequency of the TE band was chosen to correspond to a wavelength of $\lambda_c = 500$ nm. To achieve this, the normalizing wavelength was required to be $\lambda_0 = 718.38$ nm. The layer lengths were quarter-wavelengths at λ_0. The TE bandwidth calculated with `omniband` is also shown.

The Brewster angles inside the high- and low-index layers are $\theta_H = 28.52^o$ and $\theta_L = 61.48^o$. As expected, they satisfy $\theta_H + \theta_L = 90^o$.

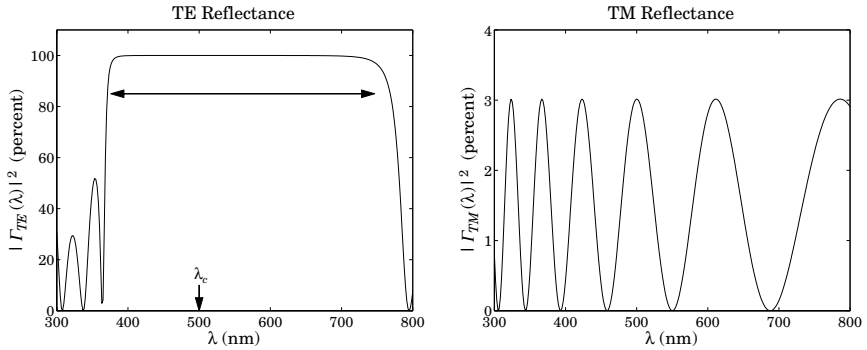

Fig. 7.6.2 Polarizer with $n_H = 2.3$ and $n_L = 1.25$.

Fig. 7.6.3 shows the second case having $n_H = 2.04$, $n_L = 1.385$, $n_a = n_b = 1.6205$. The normalizing wavelength was $\lambda_0 = 716.27$ nm in order to give $\lambda_c = 500$ nm. This case achieves a maximum TE reflectivity of 99.89% and TM reflectivity of only 0.53%. The typical MATLAB code generating these examples was:

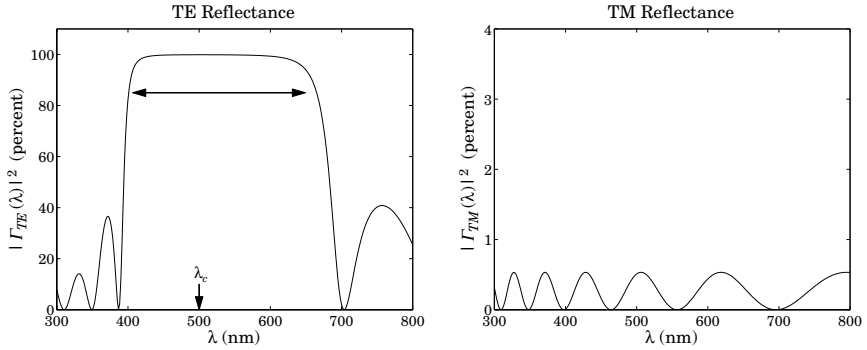

Fig. 7.6.3 Polarizer with $n_H = 2.04$ and $n_L = 1.385$.

```
nH = 2.3; nL = 1.25;
LH = 0.25; LL = 0.25;
```



```
na = nH*nL/sqrt(nH^2+nL^2)/sin(pi/4); nb=na;

[f1e,f2e] = omniband(na,nH,nL,LH,LL,th,'te',5);
lac = 500;
la0 = lac*(f1e+f2e)/2;                          because λbc = λb0/Fbc

la = linspace(300,800,301);

N = 5;
n = [na, nH, repmat([nL,nH], 1, N), nb];
L = [LH, repmat([LL,LH], 1, N)];
Ge = 100*abs(multidiel(n,L,la/la0, th, 'te')).^2;
Gm = 100*abs(multidiel(n,L,la/la0, th, 'tm')).^2;

plot(la,Ge);
```

7.7 Reflection and Refraction in Birefringent Media

Uniform plane wave propagation in biaxial media was discussed in Sec. 3.6. We found that there is an effective refractive index N such that $k = Nk_0 = N\omega/c_0$. The index N, given by Eq. (3.6.8), depends on the polarization of the fields and the direction of the wave vector. The expressions for the TE and TM fields were given in Eqs. (3.6.18) and (3.6.27).

Here, we discuss how such fields get reflected and refracted at planar interfaces between biaxial media. Further discussion can be found in [205] and [264–284].

Fig. 6.1.1 depicts the TM and TE cases, with the understanding that the left and right biaxial media are described by the triplets of principal indices $\mathbf{n} = [n_1, n_2, n_3]$ and $\mathbf{n}' = [n_1', n_2', n_3']$, and that the $\boldsymbol{E}$-fields are not perpendicular to the corresponding wave vectors in the TM case. The principal indices are aligned along the xyz axes, the xy-plane is the interface plane, and the xz-plane is the plane of incidence.

The boundary conditions require the matching of the electric field components that are tangential to the interface, that is, the components E_x in the TM case or E_y in TE. It proves convenient, therefore, to re-express Eq. (3.6.27) directly in terms of the E_x component and Eq. (3.6.18) in terms of E_y.

For the TM case, we write $\boldsymbol{E} = \hat{\mathbf{x}}\,E_x + \hat{\mathbf{z}}\,E_z = E_x(\hat{\mathbf{x}} - \hat{\mathbf{z}}\,\tan\bar{\theta})$, for the electric field of the left-incident field, where we used $E_z = -E_x \tan\bar{\theta}$. Similarly, for the magnetic field we have from Eq. (3.6.26):

$$\begin{aligned}\boldsymbol{H} &= \frac{N}{\eta_0}\,\hat{\mathbf{y}}\,(E_x\cos\theta - E_z\sin\theta) = \frac{N}{\eta_0}\,\hat{\mathbf{y}}\,E_x\cos\theta\left(1 - \frac{E_z}{E_x}\tan\theta\right)\\ &= \frac{N}{\eta_0}\,\hat{\mathbf{y}}\,E_x\cos\theta\left(1 + \frac{n_1^2}{n_3^2}\tan^2\theta\right) = \frac{N}{\eta_0}\,\hat{\mathbf{y}}\,E_x\cos\theta\left(\frac{n_3^2\cos^2\theta + n_1^2\sin^2\theta}{n_3^2\cos^2\theta}\right)\\ &= \frac{N}{\eta_0}\,\hat{\mathbf{y}}\,E_x\cos\theta\left(\frac{n_3^2 n_1^2}{N^2 n_3^2\cos^2\theta}\right) = \frac{E_x}{\eta_0}\,\frac{n_1^2}{N\cos\theta}\,\hat{\mathbf{y}}\end{aligned}$$

where we replaced $E_z/E_x = -\tan\bar{\theta} = -(n_1^2/n_3^2)\tan\theta$ and used Eq. (3.7.10). Thus,

$$\boxed{\begin{aligned}\boldsymbol{E}(\mathbf{r}) &= E_x\left(\hat{\mathbf{x}} - \hat{\mathbf{z}}\,\frac{n_1^2}{n_3^2}\,\tan\theta\right)e^{-j\,\boldsymbol{k}\cdot\mathbf{r}}\\ \boldsymbol{H}(\mathbf{r}) &= \frac{E_x}{\eta_0}\,\frac{n_1^2}{N\cos\theta}\,\hat{\mathbf{y}}\,e^{-j\,\boldsymbol{k}\cdot\mathbf{r}} = \frac{E_x}{\eta_{TM}}\,\hat{\mathbf{y}}\,e^{-j\,\boldsymbol{k}\cdot\mathbf{r}}\end{aligned}} \quad \text{(TM)} \qquad (7.7.1)$$

Similarly, we may rewrite the TE case of Eq. (3.6.18) in the form:

$$\boxed{\begin{aligned}\boldsymbol{E}(\mathbf{r}) &= E_y\hat{\mathbf{y}}\,e^{-j\,\boldsymbol{k}\cdot\mathbf{r}}\\ \boldsymbol{H}(\mathbf{r}) &= \frac{E_y}{\eta_0}\,n_2\cos\theta\,(-\hat{\mathbf{x}} + \hat{\mathbf{z}}\tan\theta)\,e^{-j\,\boldsymbol{k}\cdot\mathbf{r}} = \frac{E_y}{\eta_{TE}}\,(-\hat{\mathbf{x}} + \hat{\mathbf{z}}\tan\theta)\,e^{-j\,\boldsymbol{k}\cdot\mathbf{r}}\end{aligned}} \quad \text{(TE)} \qquad (7.7.2)$$

The propagation phase factors are:

$$\boxed{e^{-j\,\boldsymbol{k}\cdot\mathbf{r}} = e^{-jk_0xN\sin\theta - jk_0zN\cos\theta}} \quad \text{(TM and TE propagation factors)} \qquad (7.7.3)$$

Unlike the isotropic case, the phase factors are different in the TM and TE cases because the value of N is different, as given by Eq. (3.6.8), or,

$$N = \begin{cases} \dfrac{n_1 n_3}{\sqrt{n_1^2\sin^2\theta + n_3^2\cos^2\theta}}, & \text{(TM or p-polarization)}\\ n_2, & \text{(TE or s-polarization)}\end{cases} \qquad (7.7.4)$$

In Eqs. (7.7.1) and (7.7.2), the effective *transverse impedances* are defined by $\eta_{TM} = E_x/H_y$ and $\eta_{TE} = -E_y/H_x$, and are given as follows:

$$\boxed{\eta_{TM} = \eta_0\,\frac{N\cos\theta}{n_1^2}, \quad \eta_{TE} = \frac{\eta_0}{n_2\cos\theta}} \quad \text{(transverse impedances)} \qquad (7.7.5)$$

Defining the TM and TE effective *transverse refractive indices* through $\eta_{TM} = \eta_0/n_{TM}$ and $\eta_{TE} = \eta_0/n_{TE}$, we have:

$$\boxed{\begin{aligned} n_{TM} &= \frac{n_1^2}{N\cos\theta} = \frac{n_1 n_3}{\sqrt{n_3^2 - N^2\sin^2\theta}}\\ n_{TE} &= n_2\cos\theta\end{aligned}} \quad \text{(transverse refractive indices)} \qquad (7.7.6)$$

where we used Eq. (3.6.23) for the TM case, that is,

$$\boxed{N\cos\theta = \frac{n_1}{n_3}\sqrt{n_3^2 - N^2\sin^2\theta}} \qquad (7.7.7)$$

In the isotropic case, $N = n_1 = n_2 = n_3 = n$, Eqs. (7.7.6) reduce to Eq. (6.2.13). Next, we discuss the TM and TE reflection and refraction problems of Fig. 6.1.1.

Assuming that the interface is at $z = 0$, the equality of the total tangential electric fields (E_x component for TM and E_y for TE), implies as in Sec. 6.1 that the propagation phase factors must match at all values of x:

$$e^{-jk_{x+}x} = e^{-jk_{x-}x} = e^{-jk'_{x+}x} = e^{-jk'_{x-}x}$$

which requires that $k_{x+} = k_{x-} = k'_{x+} = k'_{x-}$, or, because $k_x = k\sin\theta = Nk_0\sin\theta$:

$$N\sin\theta_+ = N\sin\theta_- = N'\sin\theta'_+ = N'\sin\theta'_-$$

This implies Snell's law of reflection, that is, $\theta_+ = \theta_- \equiv \theta$ and $\theta'_+ = \theta'_- \equiv \theta'$, and Snell's law of refraction,

$$\boxed{N\sin\theta = N'\sin\theta'} \quad \text{(Snell's law for birefringent media)} \qquad (7.7.8)$$

Thus, Snell's law is essentially the same as in the isotropic case, provided one uses the effective refractive index N. Because N depends on the polarization, there will be two different refraction angles[†] for the same angle of incidence. In particular, Eq. (7.7.8) can be written explicitly in the two polarization cases:

$$\frac{n_1 n_3\sin\theta}{\sqrt{n_1^2\sin^2\theta + n_3^2\cos^2\theta}} = \frac{n'_1 n'_3\sin\theta'}{\sqrt{n_1'^2\sin^2\theta' + n_3'^2\cos^2\theta'}} \quad \text{(TM)} \qquad (7.7.9a)$$

$$n_2\sin\theta = n'_2\sin\theta' \quad \text{(TE)} \qquad (7.7.9b)$$

Both expressions reduce to Eq. (6.1.6) in the isotropic case. The explicit solutions of Eq. (7.7.9a) for $\sin\theta'$ and $\sin\theta$ are:

$$\begin{aligned}\sin\theta' &= \frac{n_1 n_3 n'_3\sin\theta}{\sqrt{[n_1'^2 n_3'^2(n_1^2 - n_3^2) - n_1^2 n_3^2(n_1'^2 - n_3'^2)]\sin^2\theta + n_1'^2 n_3'^2 n_3^2}}\\ \sin\theta &= \frac{n'_1 n'_3 n_3\sin\theta'}{\sqrt{[n_1^2 n_3^2(n_1'^2 - n_3'^2) - n_1'^2 n_3'^2(n_1^2 - n_3^2)]\sin^2\theta' + n_1^2 n_3^2 n_3'^2}}\end{aligned} \qquad (7.7.10)$$

The MATLAB function `snell`, solves Eqs. (7.7.9) for θ' given the angle of incidence θ and the polarization type. It works for any type of medium, isotropic, uniaxial, or biaxial. It has usage:

```
thb = snell(na,nb,tha,pol);          % refraction angle from Snell's law
```

The refractive index inputs `na`, `nb` may be entered as 1-, 2-, or 3-dimensional column or row vectors, for example, $\mathbf{n}_a = [n_a]$ (isotropic), $\mathbf{n}_a = [n_{ao}, n_{ae}]$ (uniaxial), or $\mathbf{n}_a = [n_{a1}, n_{a2}, n_{a3}]$ (biaxial).

Next, we discuss the propagation and matching of the transverse fields. All the results of Sec. 6.3 translate verbatim to the birefringent case, provided one uses the proper transverse refractive indices according to Eq. (7.7.6).

[†] Hence, the name birefringent.

In particular, the propagation equations (6.3.5)-(6.3.7) for the transverse fields, for the transverse reflection coefficients Γ_T, and for the transverse wave impedances Z_T, remain unchanged.

The *phase thickness* δ_z for propagating along z by a distance l also remains the same as Eq. (6.3.8), except that the index N must be used in the optical length, and therefore, δ_z depends on the polarization:

$$\boxed{\delta_z = k_z l = kl\cos\theta = Nk_0 l\cos\theta = \frac{2\pi}{\lambda} lN\cos\theta} \tag{7.7.11}$$

Using Eq. (7.7.7), we have explicitly:

$$\delta_z = \frac{2\pi}{\lambda} l\,\frac{n_1}{n_3}\sqrt{n_3^2 - N^2\sin^2\theta}\,, \qquad \text{(TM)} \tag{7.7.12a}$$

$$\delta_z = \frac{2\pi}{\lambda} l n_2\cos\theta\,, \qquad \text{(TE)} \tag{7.7.12b}$$

The transverse matching matrix (6.3.11) and Fresnel reflection coefficients (6.3.12) remain the same. Explicitly, we have in the TM and TE cases:

$$\boxed{\begin{aligned}\rho_{TM} &= \frac{n_{TM} - n'_{TM}}{n_{TM} + n'_{TM}} = \frac{\dfrac{n_1^2}{N\cos\theta} - \dfrac{n_1'^2}{N'\cos\theta'}}{\dfrac{n_1^2}{N\cos\theta} + \dfrac{n_1'^2}{N'\cos\theta'}} \\ \rho_{TE} &= \frac{n_{TE} - n'_{TE}}{n_{TE} + n'_{TE}} = \frac{n_2\cos\theta - n'_2\cos\theta'}{n_2\cos\theta + n'_2\cos\theta'}\end{aligned}} \tag{7.7.13}$$

Using Eq. (7.7.6) and the TM and TE Snell's laws, Eqs. (7.7.9), we may rewrite the reflection coefficients in terms of the angle θ only:

$$\boxed{\begin{aligned}\rho_{TM} &= \frac{n_1 n_3\sqrt{n_3'^2 - N^2\sin^2\theta} - n'_1 n'_3\sqrt{n_3^2 - N^2\sin^2\theta}}{n_1 n_3\sqrt{n_3'^2 - N^2\sin^2\theta} + n'_1 n'_3\sqrt{n_3^2 - N^2\sin^2\theta}} \\ \rho_{TE} &= \frac{n_2\cos\theta - \sqrt{n_2'^2 - n_2^2\sin^2\theta}}{n_2\cos\theta + \sqrt{n_2'^2 - n_2^2\sin^2\theta}}\end{aligned}} \tag{7.7.14}$$

The quantity $N^2\sin^2\theta$ can be expressed directly in terms of θ and the refractive indices of the incident medium. Using Eq. (7.7.4), we have:

$$\boxed{N^2\sin^2\theta = \frac{n_1^2 n_3^2\sin^2\theta}{n_1^2\sin^2\theta + n_3^2\cos^2\theta}} \tag{7.7.15}$$

The TE reflection coefficient behaves like the TE isotropic case. The TM coefficient exhibits a much more complicated behavior. If $n_1 = n'_1$ but $n_3 \neq n'_3$, it behaves like the TM isotropic case. If $n_3 = n'_3$ but $n_1 \neq n'_1$, the square-root factors cancel and it becomes independent of θ:

$$\boxed{\rho_{TM} = \frac{n_1 - n'_1}{n_1 + n'_1}} \tag{7.7.16}$$

Another interesting case is when both media are uniaxial and $n'_3 = n_1$ and $n'_1 = n_3$, that is, the refractive index vectors are $\mathbf{n} = [n_1, n_1, n_3]$ and $\mathbf{n}' = [n_3, n_3, n_1]$. It is straightforward to show in this case that $\rho_{TM} = \rho_{TE}$ at all angles of incidence. Multilayer films made from alternating such materials exhibit similar TM and TE optical properties [264].

The MATLAB function `fresnel` can evaluate Eqs. (7.7.14) at any range of incident angles θ. The function determines internally whether the media are isotropic, uniaxial, or biaxial.

7.8 Brewster and Critical Angles in Birefringent Media

The maximum angle of refraction, critical angle of incidence, and Brewster angle, have their counterparts in birefringent media.

It is straightforward to verify that θ' is an increasing function of θ in Eq. (7.7.9). The maximum angle of refraction θ'_c is obtained by setting $\theta = 90^o$ in Eq. (7.7.9).

For the TE case, we obtain $\sin\theta'_c = n_2/n'_2$. As in the isotropic case of Eq. (6.5.2), this requires that $n_2 < n'_2$, that is, the incident medium is less dense than the transmitted medium, with respect to the index n_2. For the TM case, we obtain from Eq. (7.7.9a):

$$\boxed{\sin\theta'_c = \frac{n_3 n'_3}{\sqrt{n_3^2 n_3'^2 + n_1'^2(n_3'^2 - n_3^2)}}} \qquad \text{(maximum TM refraction angle)} \tag{7.8.1}$$

This requires that $n_3 < n'_3$. On the other hand, if $n_3 > n'_3$, we obtain the critical angle of incidence θ_c that corresponds to $\theta' = 90^o$ in Eq. (7.7.10):

$$\boxed{\sin\theta_c = \frac{n_3 n'_3}{\sqrt{n_3^2 n_3'^2 + n_1^2(n_3^2 - n_3'^2)}}} \qquad \text{(critical TM angle)} \tag{7.8.2}$$

whereas for the TE case, we have $\sin\theta_c = n'_2/n_2$, which requires $n_2 > n'_2$.

In the isotropic case, a Brewster angle always exists at which the TM reflection coefficient vanishes, $\rho_{TM} = 0$. In the birefringent case, the Brewster angle does not necessarily exist, as is the case of Eq. (7.7.16), and it can also have the value zero, or even be imaginary.

The Brewster angle condition $\rho_{TM} = 0$ is equivalent to the equality of the transverse refractive indices $n_{TM} = n'_{TM}$. Using Eq. (7.7.6), we obtain:

$$n_{TM} = n'_{TM} \quad \Rightarrow \quad \frac{n_1 n_3}{\sqrt{n_3^2 - N^2\sin^2\theta}} = \frac{n'_1 n'_3}{\sqrt{n_3'^2 - N^2\sin^2\theta}} \tag{7.8.3}$$

where $N^2\sin^2\theta$ is given by Eq. (7.7.15). Solving for θ, we obtain the expression for the Brewster angle from the left medium:

$$\boxed{\tan\theta_B = \frac{n_3 n_3'}{n_1^2}\sqrt{\frac{n_1^2 - n_1'^2}{n_3^2 - n_3'^2}}} \qquad \text{(Brewster angle)} \tag{7.8.4}$$

Working instead with $N'\sin\theta' = N\sin\theta$, we obtain the Brewster angle from the right medium, interchanging the roles of the primed and unprimed quantities:

$$\boxed{\tan\theta_B' = \frac{n_3 n_3'}{n_1'^2}\sqrt{\frac{n_1^2 - n_1'^2}{n_3^2 - n_3'^2}}} \qquad \text{(Brewster angle)} \tag{7.8.5}$$

Eqs. (7.8.4) and (7.8.5) reduce to Eqs. (6.6.2) and (6.6.3) in the isotropic case. It is evident from Eq. (7.8.4) that θ_B is a real angle only if the quantity under the square root is non-negative, that is, only if $n_1 > n_1'$ and $n_3 > n_3'$, or if $n_1 < n_1'$ and $n_3 < n_3'$. Otherwise, θ_B is imaginary. In the special case, $n_1 = n_1'$ but $n_3 \neq n_3'$, the Brewster angle vanishes. If $n_3 = n_3'$, the Brewster angle does not exist, since then ρ_{TM} is given by Eq. (7.7.16) and cannot vanish.

The MATLAB function `brewster` computes the Brewster angle θ_B, as well as the critical angles θ_c and θ_c'. For birefringent media the critical angles depend on the polarization. Its usage is as follows:

```
        [thB,thc] = brewster(na,nb)          % isotropic case
[thB,thcTE,thcTM] = brewster(na,nb)          % birefringent case
```

In multilayer systems, it is convenient to know if the Brewster angle of an internal interface is accessible from the incident medium. Using Snell's law we have in this case $N_a\sin\theta_a = N\sin\theta$, where θ_a is the incident angle and N_a the effective index of the incident medium. It is simpler, then, to solve Eq. (7.8.3) directly for θ_a:

$$\boxed{N_a^2\sin^2\theta_a = N^2\sin^2\theta_B = \frac{n_3^2 n_3'^2(n_1^2 - n_1'^2)}{n_1^2 n_3^2 - n_3'^2 n_1'^2}} \tag{7.8.6}$$

Example 7.8.1: To illustrate the variety of possible Brewster angle values, we consider the following birefringent cases:

$$\begin{aligned}
&(a) \quad \mathbf{n} = [1.63, 1.63, 1.5], \quad && \mathbf{n}' = [1.63, 1.63, 1.63]\\
&(b) \quad \mathbf{n} = [1.54, 1.54, 1.63], && \mathbf{n}' = [1.5, 1.5, 1.5]\\
&(c) \quad \mathbf{n} = [1.8, 1.8, 1.5], && \mathbf{n}' = [1.5, 1.5, 1.5]\\
&(d) \quad \mathbf{n} = [1.8, 1.8, 1.5], && \mathbf{n}' = [1.56, 1.56, 1.56]
\end{aligned}$$

These cases were discussed in [264]. The corresponding materials are: (a) birefringent polyester and isotropic polyester, (b) syndiotactic polystyrene and polymethylmethacrylate (PMMA), (c) birefringent polyester and PMMA, and (d) birefringent polyester and isotropic polyester.

Because $n_1 = n_1'$ in case (a), the Brewster angle will be zero, $\theta_B = 0^\circ$. In case (b), we calculate $\theta_B = 29.4^\circ$. Because $n_2 > n_2'$ and $n_3 > n_3'$, there will be both TE and TM critical angles of reflection: $\theta_{c,TE} = 76.9^\circ$ and $\theta_{c,TM} = 68.1^\circ$.

In case (c), the Brewster angle does not exist because $n_3 = n_3'$, and in fact, the TM reflection coefficient is independent of the incident angle as in Eq. (7.7.16). The corresponding critical angles of reflection are: $\theta_{c,TE} = 56.4^\circ$ and $\theta_{c,TM} = 90^\circ$.

Finally, in case (d), because $n_2 > n_2'$ but $n_3 < n_3'$, the Brewster angle will be imaginary, and there will be a TE critical angle of reflection and a TM maximum angle of refraction: $\theta_{c,TE} = 60.1^\circ$ and $\theta_{c,TM}' = 74.1^\circ$.

Fig. 7.8.1 shows the TM and TE reflection coefficients $|\rho_{TM}(\theta)|$ of Eq. (7.7.14) versus θ in the range $0 \le \theta \le 90^\circ$.

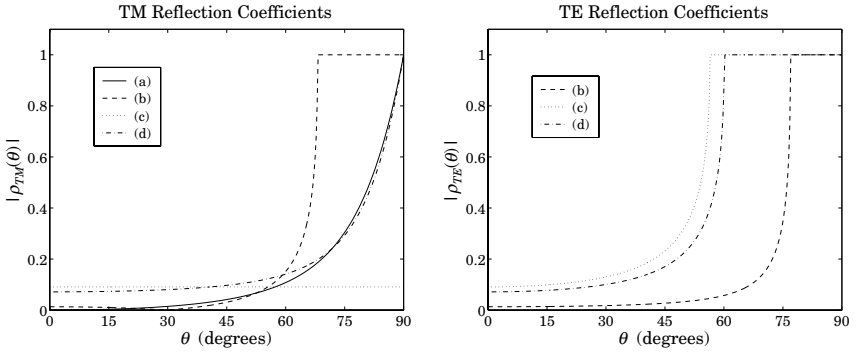

Fig. 7.8.1 TM and TE birefringent Fresnel reflection coefficients versus incident angle.

The TE coefficient in case (a) is not plotted because it is identically zero. In order to expand the vertical scales, Fig. 7.8.2 shows the TM reflectances normalized by their values at $\theta = 0^\circ$, that is, it plots the quantities $|\rho_{TM}(\theta)/\rho_{TM}(0^\circ)|^2$. Because in case (a) $\rho_{TM}(0^\circ) = 0$, we have plotted instead the scaled-up quantity $|100\rho_{TM}(\theta)|^2$.

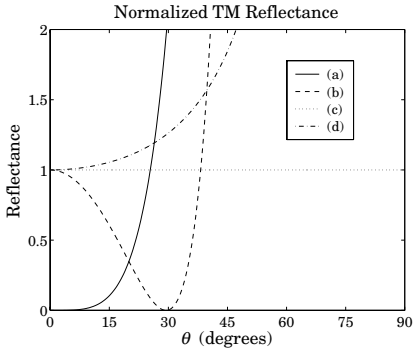

Fig. 7.8.2 TM reflectances normalized at normal incidence.

The typical MATLAB code used to compute the critical angles and generate these graphs was:

```
th = linspace(0,90,361);                          % θ at 1/4° intervals

na = [1.63,1.63,1.5]; nb = [1.63,1.63,1.63];      % note the variety of
[rte1,rtm1] = fresnel(na,nb,th);                  % equivalent ways of
[thb1,thcTE1,thcTM1] = brewster(na,nb);           % entering na and nb

na = [1.54,1.63];
nb = [1.5, 1.5];                                  % FRESNEL and BREWSTER
[rte2,rtm2] = fresnel(na,nb,th);                  % internally extend
[thb2,thcTE2,thcTM2] = brewster(na,nb);           % na,nb into 3-d arrays

na = [1.8, 1.5];                                  % same as na=[1.8,1.8,1.5]
nb = 1.5;                                         % and nb=[1.5,1.5,1.5]
[rte3,rtm3] = fresnel(na,nb,th);
[thb3,thcTE3,thcTM3] = brewster(na,nb);           % in this case, θbB = []

na = [1.8,1.5];
nb = 1.56;
[rte4,rtm4] = fresnel(na,nb,th);
[thb4,thcTE4,thcTM4] = brewster(na,nb);

plot(th, abs([rtm1; rtm2; rtm3; rtm4]));
```

We note four striking properties of the birefringent cases that have no counterparts for isotropic materials: (i) The Brewster angle can be zero, (ii) the Brewster angle may not exist, (iii) the Brewster angle may be imaginary with the TE and TM reflection coefficients both increasing monotonically with the incident angle, and (iv) there may be total internal reflection in one polarization but not in the other.

7.9 Multilayer Birefringent Structures

With some redefinitions, all the results of Sec. 7.1 on multilayer dielectric structures translate essentially unchanged to the birefringent case.

We assume the same M-layer configuration shown in Fig. 7.1.1, where now each layer is a biaxial material. The orthogonal optic axes of all the layers are assumed to be aligned with the xyz film axes. The xz-plane is the plane of incidence, the layer interfaces are parallel to the xy-plane, and the layers are arranged along the z-axis.

The ith layer is described by the triplet of refractive indices $\mathbf{n}_i = [n_{i1}, n_{i2}, n_{i3}]$, $i = 1, 2, \ldots, M$. The incident and exit media a, b may also be birefringent with $\mathbf{n}_a = [n_{a1}, n_{a2}, n_{a3}]$ and $\mathbf{n}_b = [n_{b1}, n_{b2}, n_{b3}]$, although in our examples, we will assume that they are isotropic.

The reflection/refraction angles in each layer depend on the assumed polarization and are related to each other by the birefringent version of Snell's law, Eq. (7.7.8):

$$\boxed{N_a \sin\theta_a = N_i \sin\theta_i = N_b \sin\theta_b}, \quad i = 1, 2 \ldots, M \tag{7.9.1}$$

where N_a, N_i, N_b are the effective refractive indices given by Eq. (7.7.4). The phase thickness of the ith layer depends on the polarization:

$$\delta_i = \frac{2\pi}{\lambda} l_i N_i \cos\theta_i = \begin{cases} \dfrac{2\pi}{\lambda} l_i n_{i1} \sqrt{1 - \dfrac{N_a^2 \sin^2\theta_a}{n_{i3}^2}}, & \text{(TM)} \\ \dfrac{2\pi}{\lambda} l_i n_{i2} \sqrt{1 - \dfrac{N_a^2 \sin^2\theta_a}{n_{i2}^2}}, & \text{(TE)} \end{cases} \tag{7.9.2}$$

where we used Eq. (7.7.7) and Snell's law to write in the TM and TE cases:

$$N_i \cos\theta_i = \begin{cases} \dfrac{n_{i1}}{n_{i3}} \sqrt{n_{i3}^2 - N_i^2 \sin^2\theta_i} = n_{i1} \sqrt{1 - \dfrac{N_i^2 \sin^2\theta_i}{n_{i3}^2}} = n_{i1} \sqrt{1 - \dfrac{N_a^2 \sin^2\theta_a}{n_{i3}^2}} \\ n_{i2} \cos\theta_i = n_{i2} \sqrt{1 - \sin^2\theta_i} = n_{i2} \sqrt{1 - \dfrac{N_a^2 \sin^2\theta_a}{n_{i2}^2}} \end{cases}$$

To use a unified notation for the TM and TE cases, we define the layer optical lengths at normal-incidence, normalized by a fixed free-space wavelength λ_0:

$$L_i = \begin{cases} \dfrac{l_i n_{i1}}{\lambda_0}, & \text{(TM)} \\ \dfrac{l_i n_{i2}}{\lambda_0}, & \text{(TE)} \end{cases}, \quad i = 1, 2, \ldots, M \tag{7.9.3}$$

We define also the cosine coefficients c_i, which represent $\cos\theta_i$ in the TE birefringent case and in the TM isotropic case:

$$c_i = \begin{cases} \sqrt{1 - \dfrac{N_a^2 \sin^2\theta_a}{n_{i3}^2}}, & \text{(TM)} \\ \sqrt{1 - \dfrac{N_a^2 \sin^2\theta_a}{n_{i2}^2}}, & \text{(TE)} \end{cases}, \quad i = 1, 2, \ldots, M \tag{7.9.4}$$

At normal incidence the cosine factors are unity, $c_i = 1$. With these definitions, Eq. (7.9.2) can be written compactly in the form:

$$\boxed{\delta_i = 2\pi \frac{\lambda_0}{\lambda} L_i c_i = 2\pi \frac{f}{f_0} L_i c_i}, \quad i = 1, 2, \ldots, M \tag{7.9.5}$$

where λ is the operating free-space wavelength and $f = c_0/\lambda$, $f_0 = c_0/\lambda_0$. This is the birefringent version of Eq. (7.1.10). A typical design might use quarter-wave layers, $L_i = 1/4$, at λ_0 and at normal incidence.

The reflection coefficients ρ_{Ti} at the interfaces are given by Eq. (7.1.3), but now the transverse refractive indices are defined by the birefringent version of Eq. (7.1.4):

$$n_{Ti} = \begin{cases} \dfrac{n_{i1}^2}{N_i \cos\theta_i} = \dfrac{n_{i1} n_{i3}}{\sqrt{n_{i3}^2 - N_a^2 \sin^2\theta_a}}, & \text{(TM)} \\ n_{i2} \cos\theta_i = \sqrt{n_{i2}^2 - N_a^2 \sin^2\theta_a}, & \text{(TE)} \end{cases}, \quad i = a, 1, 2, \ldots, M, b \tag{7.9.6}$$

With the above redefinitions, the propagation and matching equations (7.1.5)–(7.1.9) remain unchanged. The MATLAB function `multidiel` can also be used in the birefringent case to compute the frequency reflection response of a multilayer structure. Its usage is still:

```
[Gamma1,Z1] = multidiel(n,L,lambda,theta,pol);      % birefringent multilayer structure
```

where the input `n` is a $1\times(M+2)$ vector of refractive indices in the isotropic case, or a $3\times(M+2)$ matrix, where each column represents the triplet of birefringent indices of each medium. For uniaxial materials, `n` may be entered as a $2\times(M+2)$ matrix.

7.10 Giant Birefringent Optics

The results of Sec. 7.5 can be applied almost verbatim to the birefringent case. In Fig. 7.5.1, we assume that the high and low alternating layers are birefringent, described by the triplet indices $\mathbf{n}_H = [n_{H1}, n_{H2}, n_{H3}]$ and $\mathbf{n}_L = [n_{L1}, n_{L2}, n_{L3}]$. The entry and exit media may also be assumed to be birefringent. Then, Snell's laws give:

$$N_a \sin\theta_a = N_H \sin\theta_H = N_L \sin\theta_L = N_b \sin\theta_b \tag{7.10.1}$$

The phase thicknesses δ_H and δ_L within the high and low index layers are:

$$\boxed{\delta_H = 2\pi \frac{f}{f_0} L_H c_H\,, \quad \delta_L = 2\pi \frac{f}{f_0} L_L c_L} \tag{7.10.2}$$

where L_H, c_H and L_L, c_L are defined by Eqs. (7.9.3) and (7.9.4) for $i = H, L$. The effective transverse refractive indices within the high and low index layers are given by Eq. (7.9.6), again with $i = H, L$.

The alternating reflection coefficient ρ_T between the high/low interfaces is given by Eq. (7.7.14), with the quantity $N^2\sin^2\theta$ replaced by $N_a^2\sin^2\theta_a$ by Snell's law:

$$\boxed{\begin{aligned}
\rho_{TM} &= \frac{n_{H1}n_{H3}\sqrt{n_{L3}^2 - N_a^2\sin^2\theta_a} - n_{L1}n_{L3}\sqrt{n_{H3}^2 - N_a^2\sin^2\theta_a}}{n_{H1}n_{H3}\sqrt{n_{L3}^2 - N_a^2\sin^2\theta_a} + n_{L1}n_{L3}\sqrt{n_{H3}^2 - N_a^2\sin^2\theta_a}} \\
\rho_{TE} &= \frac{\sqrt{n_{H2}^2 - N_a^2\sin^2\theta_a} - \sqrt{n_{L2}^2 - N_a^2\sin^2\theta_a}}{\sqrt{n_{H2}^2 - N_a^2\sin^2\theta_a} + \sqrt{n_{L2}^2 - N_a^2\sin^2\theta_a}}
\end{aligned}} \tag{7.10.3}$$

The multilayer structure will exhibit reflection bands whose bandedges can be calculated from Eqs. (7.5.7)–(7.5.17), with the redefinition $L_\pm = L_H c_H \pm L_L c_L$. The MATLAB function `omniband2` calculates the bandedges. It has usage:

```
[F1,F2] = omniband2(na,nH,nL,LH,LL,th,pol,N);
```

where `pol` is one of the strings `'te'` or `'tm'` for TE or TM polarization, and `na`, `nH`, `nL` are 1-d, 2-d, or 3-d row or column vectors of birefringent refractive indices.

Next, we discuss some mirror design examples from [264] that illustrate some properties that are specific to birefringent media. The resulting optical effects in such mirror structures are referred to as *giant birefringent optics* (GBO) in [264,850].

Example 7.10.1: We consider a GBO mirror consisting of 50-bilayers of high and low index quarter-wave layers with refractive indices $\mathbf{n}_H = [1.8, 1.8, 1.5]$, $\mathbf{n}_L = [1.5, 1.5, 1.5]$ (birefringent polyester and isotropic PMMA.) The surrounding media are air, $n_a = n_b = 1$.

The layers are quarter wavelength at the normalization wavelength $\lambda_0 = 700$ nm at normal incidence, so that for both polarizations we take $L_H = L_L = 1/4$.

Because the high/low index layers are matched along the z-direction, $n_{H3} = n_{L3}$, the TM reflection coefficient at the high/low interface will be constant, independent of the incident angle θ_a, as in Eq. (7.7.16). However, some dependence on θ_a is introduced through the cosine factors c_H, c_L of Eq. (7.10.2).

The left graph of Fig. 7.10.1 shows the reflectance $|\Gamma_T(\lambda)|^2$ as a function of λ for an angle of incidence $\theta_a = 60^o$. The TM and TE bandedge wavelengths were calculated from `omniband2` to be: $[\lambda_1, \lambda_2] = [540.24, 606.71]$ and $[\lambda_1, \lambda_2] = [548.55, 644.37]$ nm.

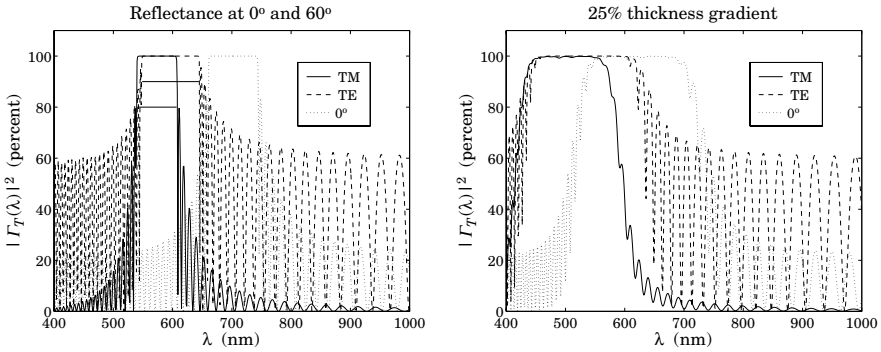

Fig. 7.10.1 Reflectance of birefringent mirror.

The typical MATLAB code used to generate the left graph and the bandedge wavelengths was as follows:

```
LH = 0.25; LL = 0.25;

na = [1; 1; 1];
nH = [1.8; 1.8; 1.5];
nL = [1.5; 1.5; 1.5];
nb = [1; 1; 1];

la0 = 700;
la = linspace(400,1000,601);

th = 60;                                        % angle of incidence

N = 50;                                         % number of bilayers
n = [na, repmat([nH,nL], 1, N), nb];            % 3×(2N + 2) matrix
L = [repmat([LH,LL], 1, N)];
```

```
Ge = 100*abs(multidiel(n, L, la/la0, th, 'te')).^2;
Gm = 100*abs(multidiel(n, L, la/la0, th, 'tm')).^2;
G0 = 100*abs(multidiel(n, L, la/la0)).^2;

plot(la,Gm,'-', la,Ge,'--', la,G0,':');

[F1,F2]=omniband2(na,nH,nL,LH,LL,th,'tm',3);
la1 = la0/F2;  la2 = la0/F1;                    % TM bandedge wavelengths
```

The right graph shows the reflectance with a 25% thickness gradient (the layer thicknesses L_H, L_L decrease linearly from quarter-wavelength to 25% less than that at the end.) This can be implemented in MATLAB by defining the thickness vector L by:

```
L = [repmat([LH,LL], 1, N)];
L = L .* (1 - linspace(0, 0.25, 2*N));    % 25% thickness gradient
```

The thickness gradient increases the effective bandwidth of the reflecting bands [263]. However, the bandwidth calculation can no longer be done with `omniband2`. The band centers can be shifted to higher wavelengths by choosing λ_0 higher. The reflecting bands can be made flatter by increasing the number of bilayers. □

Example 7.10.2: In this example, we design a 30-bilayer GBO mirror with $\mathbf{n}_H = [1.8, 1.8, 1.5]$ and $\mathbf{n}_L = [1.5, 1.5, 1.8]$, so that $n_{H1} = n_{H2} = n_{L3}$ and $n_{H3} = n_{L1} = n_{L2}$. As we discussed in Sec. 7.7, it follows from Eq. (7.7.14) that $\rho_{TM} = \rho_{TE}$ for all angles of incidence.

As in Ref. [264], the media a, b are taken to be isotropic with $n_a = n_b = 1.4$. The normalization wavelength at which the high/low index layer are quarter-wavelength is $\lambda_0 = 700$ nm.

The left graph of Fig. 7.10.2 shows the reflectance for a 45° angle of incidence. Because $\rho_{TM} = \rho_{TE}$, the reflection bands for the TM and TE cases are essentially the same.

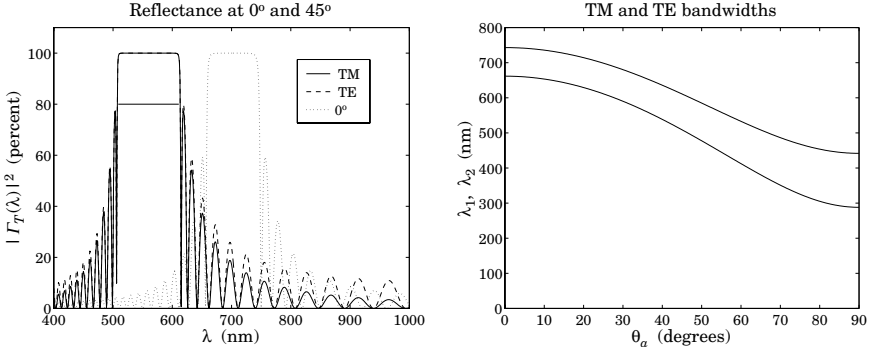

Fig. 7.10.2 Birefringent mirror with identical TM and TE reflection bands.

The right graph depicts the asymptotic (for large number of bilayers) bandedges of the reflecting band versus incident angle. They were computed with `omniband2`. Unlike the isotropic case, the TM and TE bands are exactly identical. This is a consequence of the

following relationships between the cosine factors in this example: $c_{H,TM} = c_{L,TE}$ and $c_{H,TE} = c_{L,TM}$. Then, because we assume quarter-wave layers in both the TE and TM cases, $L_H = L_L = 1/4$, we will have:

$$L_{+,TM} = L_{H,TM}c_{H,TM} + L_{L,TM}c_{L,TM} == \frac{1}{4}(c_{H,TM} + c_{L,TM}) = \frac{1}{4}(c_{L,TE} + c_{H,TE}) = L_{+,TE}$$

$$L_{-,TM} = L_{H,TM}c_{H,TM} - L_{L,TM}c_{L,TM} == \frac{1}{4}(c_{H,TM} - c_{L,TM}) = \frac{1}{4}(c_{L,TE} - c_{H,TE}) = -L_{+,TE}$$

Because the computational algorithm (7.5.17) for the bandwidth does not depend on the sign of L_-, it follows that Eq. (7.5.17) will have the same solution for the TM and TE cases. The typical MATLAB code for this example was:

```
LH = 0.25; LL = 0.25;

na = [1.4; 1.4; 1.4];
nb = [1.4; 1.4; 1.4];
nH = [1.8; 1.8; 1.5];
nL = [1.5; 1.5; 1.8];

la0 = 700;
la = linspace(400,1000,601);

tha = 45;

N = 30;
n = [na, repmat([nH,nL], 1, N), nb];
L = [repmat([LH,LL], 1, N)];

Ge = 100*abs(multidiel(n, L, la/la0, tha, 'te')).^2;
Gm = 100*abs(multidiel(n, L, la/la0, tha, 'tm')).^2;
G0 = 100*abs(multidiel(n, L, la/la0)).^2;

plot(la,Gm,'-', la,Ge,'--', la,G0,':');
```

In Fig. 7.10.3, the low-index material is changed slightly to $\mathbf{n}_L = [1.5, 1.5, 1.9]$. The main behavior of the structure remains the same, except now the TM and TE bands are slightly different.

The MATLAB code used to compute the right graph was:

```
theta = linspace(0,90,361);                          % incident angles

F1e = []; F2e = [];
F1m = []; F2m = [];

Ni = 3;                                              % refinement iterations

for i=1:length(theta),
  [f1e,f2e] = omniband2(na,nH,nL,LH,LL,theta(i),'te',Ni);
  [f1m,f2m] = omniband2(na,nH,nL,LH,LL,theta(i),'tm',Ni);
  F1e = [F1e,f1e]; F2e = [F2e,f2e];
  F1m = [F1m,f1m]; F2m = [F2m,f2m];                  % frequency bandedges
end
```

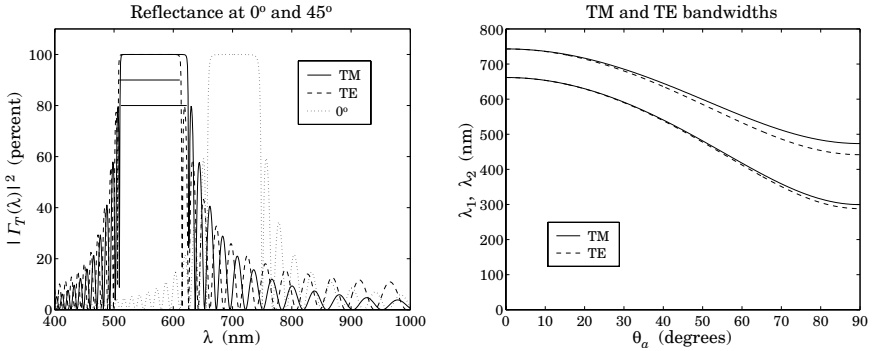

Fig. 7.10.3 Birefringent mirror with slightly different TM and TE reflection bands.

```
la1e = la0 ./ F2e; la2e = la0 ./ F1e;                    % wavelength bandedges
la1m = la0 ./ F2m; la2m = la0 ./ F1m;

plot(theta,la1m,'-', theta,la2m,'-', theta,la1e,'--', theta,la2e,'--');
```

As the incident angle increases, not only does the TM band widen but it also becomes wider than the TE band—exactly the opposite behavior from the isotropic case. □

Example 7.10.3: *GBO Reflective Polarizer.* By choosing biaxial high/low layers whose refractive indices are mismatched only in the x or the y direction, one can design a mirror structure that reflects only the TM or only the TE polarization.

Fig. 7.10.4 shows the reflectance of an 80-bilayer mirror with $\mathbf{n}_H = [1.86, 1.57, 1.57]$ for the left graph, and $\mathbf{n}_H = [1.57, 1.86, 1.57]$ for the right one. In both graphs, the low index material is the same, with $\mathbf{n}_L = [1.57, 1.57, 1.57]$.

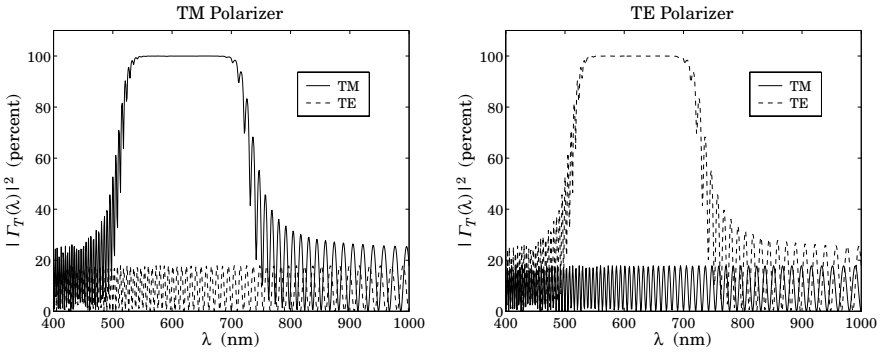

Fig. 7.10.4 TM and TE mirror polarizers.

The angle of incidence was $\theta_a = 0^\circ$. The typical MATLAB code was:


```
LH = 0.25; LL = 0.25;

na = [1; 1; 1];
nb = [1; 1; 1];
nH = [1.86; 1.57; 1.57];
nL = [1.57; 1.57; 1.57];

la0 = 700;
la = linspace(400,1000,601);

N = 80;
n = [na, repmat([nH,nL], 1, N), nb];
L = [repmat([LH,LL], 1, N)];
L = L .* linspace(1,0.75,2*N);                           % 25% thickness gradient

Ge = 100*abs(multidiel(n, L, la/la0, 0, 'te')).^2;
Gm = 100*abs(multidiel(n, L, la/la0, 0, 'tm')).^2;

plot(la,Gm,'-', la,Ge,'--');
```

A 25% thickness gradient was assumed in both cases. In the first case, the x-direction indices are different and the structure will act as a mirror for the TM polarization. The TE polarization will be reflected only by the air-high interface.

In the second case, the materials are matched in their y-direction indices and therefore, the structure becomes a mirror for the TE polarization, assuming as always that the plane of incidence is still the xz plane. □

Giant birefringent optics is a new paradigm in the design of multilayer mirrors and polarizers [264], offering increased flexibility in the control of reflected light. The recently manufactured *multilayer optical film* by 3M Corp. [850] consists of hundreds to thousands of birefringent polymer layers with individual thicknesses of the order of a wavelength and total thickness of a sheet of paper. The optical working range of such films are between 400–2500 nm.

Applications include the design of efficient waveguides for transporting visible light over long distances and piping sunlight into interior rooms, reflective polarizers for improving liquid crystal displays, and other products, such as various optoelectronic components, cosmetics, and "hot" and "cold" mirrors for architectural and automotive windows.

7.11 Problems